

# Modeling Joint Abundance of Multiple Species Using Dirichlet Process Random Effects

Devin S. Johnson<sup>1</sup> and Elizabeth H. Sinclair

Alaska Fisheries Science Center, National Marine Fisheries Service, NOAA,  
Seattle, Washington, U.S.A.

May 30, 2016

---

<sup>1</sup>Email: [devin.johnson@noaa.gov](mailto:devin.johnson@noaa.gov)

## Abstract

1 We present a method for modeling multiple species distributions simultaneously using Dirich-  
2 let Process random effects to cluster species into guilds. Guilds are ecological groups of  
3 species that behave or react similarly to some environmental conditions. By modeling latent  
4 guild structure, we capture the cross-correlations in abundance or occurrence of species over  
5 surveys. In addition, ecological information about the community structure is obtained as  
6 a byproduct of the model. By clustering species into similar functional groups, prediction  
7 uncertainty of community structure at additional sites is reduced over treating each species  
8 separately. The method is illustrated with a small simulation demonstration, as well as an  
9 analysis of a mesopelagic fish survey from the eastern Bering Sea near Alaska. The simula-  
10 tion data analysis shows that guild membership can be extracted as the differences between  
11 groups become larger and if guild differences are small the model naturally collapses all the  
12 species into a small number of guilds which increases predictive efficiency by reducing the  
13 number of parameters to that which is supported by the data.

14 **Key words:** Abundance, Dirichlet Process, Joint species distribution model, Multivariate,  
15 occurrence

## 16 1 Introduction

17 In recent years there has been considerable development of methodology for modeling and  
18 predicting abundance and occurrence of species of interest. Much of this development uses  
19 a hierarchical framework for developing models to fit the complexities of the observed data  
20 or natural abundance processes (Cressie et al., 2009; Royle and Dorazio, 2008; Hobbs and  
21 Hooten, 2015). Some of these complexities may include: spatial and temporal dependence  
22 (Carroll et al., 2010; Latimer et al., 2009; Johnson et al., 2013b; Thorson et al., 2015; Ward

23 et al., 2010), nondetection of individuals at sampled sites (Dorazio and Connor, 2014; Royle,  
24 2004), and zero-inflation (Johnson and Fritz, 2014). Many of these species distribution  
25 models (SDMs) were used to make inference to a single species or one-at-a-time modeling if  
26 community inference was desired. However, by not recognizing the fact that species interact,  
27 use of single species models for making inference for community abundance and structure  
28 can produce misleading results (Clark et al., 2014). Hence, new joint species distribution  
29 models (JSDMs), which explicitly model species interactions (or, cross-correlation) have  
30 recently been developed (e.g., Dorazio and Connor, 2014; Latimer et al., 2009; Thorson  
31 et al., 2015). Herein, we propose a novel JSDM approach which models species interactions  
32 through membership in a latent ecological guild (Simberloff and Dayan, 1991) or functional  
33 group within the sampled range of habitats.

34 Typically, description of an abundance model begins with a GLM structure for the abun-  
35 dance process using a discrete value distribution such as Poisson or negative-binomial. For  
36 example one might model the abundance as a Poisson observation with log-mean being a  
37 function of covariates that might include habitat variables or variables related to the sampling  
38 procedure which are thought to be related to the observed abundance. Alternatively, one  
39 might log transform the abundance and use Gaussian linear models (Johnson et al., 2013b;  
40 Johnson and Fritz, 2014; Ward et al., 2010), but the general mean structure is usually the  
41 same. Herein, we will focus on the GLM versions. The focus of the abundance modeling is  
42 related to either establishing an ecological relationship between (joint) abundance and the  
43 environmental covariates or predicting abundance at unsampled locations.

44 To extend the single species GLM oriented model to account for interactions of multiple  
45 species and improve prediction and inference of community structure and joint abundance,  
46 there have been several approaches which differ in the details of interaction modeling, but  
47 all fit the GLM framework by adding random effects which are either directly correlated

48 between species (Clark et al., 2014; Dorazio and Connor, 2014; Latimer et al., 2009) or when  
49 marginalized from the (log-linear) model imply a cross-species correlation structure (Thorson  
50 et al., 2015). The direct approach of using a free parameter for every pair of species when  
51 modeling the species-level correlation has been successfully implemented (Clark et al., 2014;  
52 Latimer et al., 2009), however, in those studies there were a high number of sights sampled  
53 or a low number of species considered. In other studies, unstructured covariance did not  
54 produce reliable results (Dorazio and Connor, 2014). Thus, recent efforts to contribute novel  
55 methodology for JSDMs have focused on reducing the number of parameters used to model  
56 species interactions. Dorazio and Connor (2014) used a known species trait proximity matrix  
57 to model the species-level covariance matrix using a spatial correlation function. By using the  
58 known information on species similarity there are only two parameters necessary to model  
59 the cross-correlation. Another low complexity approach has been proposed by Thorson et al.  
60 (2015) using linear combinations of latent random effects. Specifically, the latent effects are  
61 spatial fields, but the same methodology could be applied using independent random effects.  
62 If the number of random effects is small relative to the number of species modeled, the  
63 number of parameters necessary for modeling species cross-correlation can be significantly  
64 reduced from the unstructured scenario.

65 As a novel alternative, we propose an JSDM that uses latent ecological guilds to model  
66 interactions among species and obtain joint abundance inference. Herein, we also consider  
67 joint species occurrence as well, where occurrence is defined as the binary presence (i.e.,  
68 abundance  $> 0$ ) or absence (abundance = 0) of a species. Dorazio and Connor (2014) used  
69 known guild membership of different species to model independence of some species in a  
70 cross-correlated JSDM. Simberloff and Dayan (1991) defines an ecological guild to be “a  
71 group of species that exploit the same class of environmental resources in a similar way.”  
72 With this definition in mind, we seek to build a model where species are cross-correlated in

73 abundance because there are unknown group effects for some set of covariates, i.e., if the  
74 group (guild) structure was known they could be represented by (group  $\times$  covariate) inter-  
75 action terms in the abundance GLM models. To accomplish this task we format the model  
76 as a latent class or mixture model (see McLachlan and Peel, 2004). Mixture models or latent  
77 class models are often used to model dependence between variables in a nonparametric fash-  
78 ion because for a sufficiently large number of groups, marginalizing over the random latent  
79 classes can approximate any dependence structure to whatever degree desired (McLachlan  
80 and Peel, 2004; Vermunt et al., 2008). It has been shown that this holds even when the  
81 conditional models are independent given group membership (Dunson and Xing, 2009). In  
82 an ecological abundance context, finite mixture models have been used in the past to model  
83 spatial heterogeneity and correlation in a nonparametric fashion (Dorazio et al., 2008; John-  
84 son et al., 2013b). In this paper we take inspiration from nonparametric dependence methods  
85 used for spatial association and apply it to species interaction in abundance modeling.

86 In the following section we describe the general infinite mixture framework using latent  
87 classes and describe the Dirichlet Process (DP) for modeling class membership and the  
88 number of classes. There are several choices of models for number and assignment of latent  
89 classes, but we utilize the DP due to its long history and good clustering properties (Casella  
90 et al., 2014). Parameter estimation in the DP-JSDM is challenging due to the latent class  
91 process. We provide a reversible-jump MCMC (RJMCMC; Green 2003) algorithm for making  
92 Bayesian inference. Finally, we apply the method to few simulated data sets, as well as, a  
93 real data set on mesopelagic fish communities in the eastern Bering Sea, Alaska.

## 94 2 Methods

### 95 2.1 General model framework

96 We begin the description of the proposed methods with some notation. First we assume there  
97 are  $J$  surveys, for which abundance (or count index; hereafter we use the term “counts”) of  
98  $I$  different species is measured. Let  $n_{ij}$  be the observed count for  $i$ th species in survey  $j$ . We  
99 also use the vector notation  $\mathbf{n}_i = (n_{i1}, \dots, n_{iJ})'$  and  $\mathbf{n} = (\mathbf{n}'_1, \dots, \mathbf{n}'_J)'$  for the  $n_{ij}$ , as well as,  
100 other quantities described later. For occurrence modeling we denote occurrence as  $y_{ij} = 1$  if  
101  $n_{ij} > 0$  otherwise  $y_{ij} = 0$ . In practice,  $n_{ij}$  need not necessarily be observed for occurrence  
102 modeling. The notation  $\mathbf{y}_i$  and  $\mathbf{y}$  are similar to the abundance counterparts.

103 For abundance modeling, there are several possible distributions that could be used to  
104 model the observed discrete counts, Poisson, negative binomial, zero-inflated Poisson, etc., so  
105 we will generically denote this observation model as  $[n_{ij}|z_{ij}, \boldsymbol{\gamma}]$  where  $z_{ij}$  is a latent Gaussian  
106 variable controlling the level of expected abundance and  $\boldsymbol{\gamma}$  is a set of, possibly nuisance,  
107 parameters. The notation “[ $A|B$ ]” refers to the conditional distribution of  $A$  given  $B$ . For  
108 example, if a Poisson distribution is used

$$109 \quad [n_{ij}|z_{ij}, \boldsymbol{\gamma}] = \text{Poisson}(n_{ij}|e^{z_{ij}}), \quad (1)$$

110 and  $\boldsymbol{\gamma}$  is not necessary. In the example analysis of mesopelagic fish surveys we utilize a  
111 zero-inflated Poisson (ZIP) model, so,

$$112 \quad [n_{ij}|z_{ij}, \boldsymbol{\gamma}] = \gamma_{ij}1_{[n_{ij}=0]} + (1 - \gamma_{ij})\text{Poisson}(n_{ij}|e^{z_{ij}}), \quad (2)$$

113 the additional  $\gamma_{ij}$  parameter is the mixing probability for the extra zeros. For occurrence  
114 modeling we use

$$115 \quad [y_{ij}|z_{ij}] = \text{Bernoulli}(\Phi^{-1}\{z_{ij}\}), \quad (3)$$

116 where  $\Phi(\cdot)$  is the standard normal CDF, that is, a probit link function.

117 To account for unknown interspecies correlations we take a clustering approach inspired  
 118 by the analysis of Johnson et al. (2013b) for incorporating spatial structure when there  
 119 are no reasonable distance metrics or neighborhood groupings are unknown. The model is  
 120 constructed by envisioning an unknown partition,  $p$ , of the species into  $\kappa_p$  groups such that  
 121 species within groups (clusters) behave similarly with respect to the abundance process. For  
 122 a given  $p$ , we model (in vector form) the latent  $\mathbf{z}$  process with the linear model

$$123 \quad [\mathbf{z}|p, \boldsymbol{\delta}_p, \boldsymbol{\beta}, \sigma] = N(\mathbf{X}\boldsymbol{\beta} + \mathbf{K}_p\boldsymbol{\delta}_p, \boldsymbol{\Sigma}), \quad (4)$$

124 where

- 125 •  $\mathbf{X}$  is a design matrix of covariates for which there are no group-level effects,
- 126 •  $\boldsymbol{\beta}$  is a vector of regression coefficients,
- 127 •  $\mathbf{K}_p = \mathbf{C}_p \otimes \mathbf{H}$ , where  $\mathbf{C}_p$  is an  $I \times \kappa_p$  binary matrix indicating which species belong  
 128 to each group in  $p$  and  $\mathbf{H}$  is a  $J \times q$  matrix of  $q$  habitat covariates recorded at the  $j$ th  
 129 survey,
- 130 •  $\boldsymbol{\delta}_p = (\boldsymbol{\delta}'_1, \dots, \boldsymbol{\delta}'_{\kappa_p})'$  is a vector of normally distributed random effects, where,  $[\boldsymbol{\delta}_k|\boldsymbol{\Omega}] =$   
 131  $\mathcal{N}(\mathbf{0}, \boldsymbol{\Omega})$ , for  $k = 1, \dots, \kappa_p$ .
- 132 •  $\boldsymbol{\Sigma}$  is a diagonal matrix with entries  $\sigma_{ij}^2$  (for occurrence modeling  $\sigma_{ij} = 1$ ).

133 To reduce the parameter complexity of the proposed model we suggest the following for  
 134 general practice:

- 135 (i) for abundance models, set  $\boldsymbol{\sigma} = \text{diag}(\boldsymbol{\Sigma}^{1/2}) = \exp\{\mathbf{L}\boldsymbol{\theta}\}$ , where  $\mathbf{L}$  is a matrix of design  
 136 covariates and
- 137 (ii) set  $\boldsymbol{\Omega} = \omega^2(\mathbf{H}'\mathbf{H})^{-1}$ , where  $\omega = \exp(\xi)$ .

138 With respect to (i), there are some useful special cases, namely,  $\mathbf{L} = \mathbf{1}$  gives  $\sigma_{ij} = \sigma$  and  
139  $\mathbf{L} = \mathbf{I}_I \otimes \mathbf{1}_J$  gives  $\sigma_{ij} = \sigma_i$ . However, the overdispersion parameters could also be modeled  
140 based on covariates associated with sampling methods, etc. Suggestion (ii) was formulated  
141 from the covariances of the  $g$ -prior (Tiao and Zellner, 1964). The  $g$ -prior,  $N(\mathbf{0}, \omega^2(\mathbf{H}'\mathbf{H})^{-1})$ ,  
142 is an often used prior for regression coefficient parameters. It has the nice benefit that, with  
143 a single parameter, it automatically controls the scale of variance and covariance for each  
144 coefficient based on the scale of the covariates and their cross-correlation. The exponential  
145 reparameterization is used for ease of inference, that is  $\xi$  can be unconstrained.

146 The previous description assumed that the correct partitioning of the species is known,  
147 however, for most real data sets, the correct partition is unknown. Thus, we must also pro-  
148 vide a probability model over partitions,  $[p|\alpha]$ , such that marginalization over the unknown  
149 partitions creates random coefficient vectors that are nonparametric in their distribution.  
150 A commonly used distribution over partitions is the Chinese Restaurant Process (CRP) a  
151 finite number of individuals to an unknown number of groups is described as follows, for a  
152 given parameter  $\alpha > 0$ ,

- 153 1. A customer enters the restaurant and sits at one of an infinite number of tables.
- 154 2. The next customer enters and chooses to sit at the occupied table with probability  
155  $1/(1 + \alpha)$  or a new table with probability  $\alpha/(1 + \alpha)$ .
- 156 3. In general, the  $i + 1$  customer sits at an occupied table with probability proportional to  
157 the number of customers already seated or chooses an unoccupied table with probability  
158 proportional to  $\alpha$ .

159 Under the CRP model individuals are exchangeable, i.e., individuals join clusters based only  
160 on how many other individuals are in the cluster, not who else is in the cluster. This fact  
161 forms the basis for Bayesian inference for the CRP model via MCMC (Neal, 2000). The



162 density function for the CRP cluster model is given by,

$$163 \quad [p|\alpha] = \mathcal{CRP}(\alpha) \propto \frac{\Gamma(\alpha)}{\Gamma(\alpha + I)} \alpha^{\kappa_p} \prod_{k=1}^{\kappa_p} (g_{pk} - 1)!, \quad (5)$$

164 where  $g_{pk}$  is the size of the  $k$ th cluster (group) in  $p$ . Note, that the distribution of  $p$  is only  
 165 a function of the number and sizes of the groups. Realizations of  $p$  with the same number  
 166 of groups and groups sizes have the same probability regardless of which individuals fall in  
 167 which cluster.

168 The Dirichlet process is connected to the CRP process because a DP process is con-  
 169 structed using the same procedure to seat the guests in the CRP model. Specifically, in  
 170 terms of (4), let  $\bar{\delta}_i$  be the coefficient associated with the  $i$ th species, that is  $\bar{\delta}_i = \sum_{k=1}^{\kappa_p} C_{ik} \delta_k$ ,  
 171 where  $C_{ik}$  is the  $(i, k)$  entry of the  $\mathbf{C}_p$  matrix. Now, if  $\bar{\delta}_i$  follows a DP then, conditionally,

$$172 \quad [\bar{\delta}_i | \bar{\delta}_1, \dots, \bar{\delta}_{i-1}, \alpha, \Omega] = \frac{\alpha}{\alpha + i - 1} \mathcal{N}(\mathbf{0}, \Omega) + \sum_{k=1}^{u_i} \frac{n_k}{\alpha + i - 1} \delta_k, \quad (6)$$

173 where  $u_i$  is the number of unique values,  $\delta_k$ , of  $\bar{\delta}_{i'}$   $i' = 1, \dots, i - 1$ , and  $n_k$  is the number  
 174 of species 1 through  $i - 1$  belonging to group  $k$ . In other words, a new table is represented  
 175 by a new value of  $\delta_k$ . Thus, the CRP partitioning combined with the  $\delta$  realizations for each  
 176 group implies that  $[\bar{\delta}_i | \alpha, \Omega] = \mathcal{DP}(\alpha, \Omega)$ .

177 Like the spatial covariance model use by Dorazio and Connor (2014), the DP-JSDM  
 178 also marginally possesses generally positive cross-covariance structure. This makes intuitive  
 179 sense as one is clustering similar species together or, if species are dissimilar, allowing them  
 180 to be independent. The covariance structure of the DP-JSDM can be derived by forming an  
 181 intercept random effect,  $\boldsymbol{\eta} = \mathbf{K}_p \boldsymbol{\delta}_p$ , such that  $\mathbf{z} = \mathbf{X}\boldsymbol{\beta} + \boldsymbol{\eta} + \boldsymbol{\epsilon}$ , where  $[\boldsymbol{\epsilon}] = N(\mathbf{0}, \boldsymbol{\Sigma})$ . Then,  
 182 conditioning on the cluster assignment, the covariance matrix of the random effect  $\boldsymbol{\eta}$  is,

$$183 \quad \text{Var}(\boldsymbol{\eta}|p) = \mathbf{C}_p \mathbf{C}'_p \otimes \mathbf{H}\boldsymbol{\Omega}\mathbf{H}', \quad (7)$$

184 and the marginal variance is given by the mixture,

$$185 \quad \text{Var}(\boldsymbol{\eta}) = \left\{ \sum_p \mathbf{C}_p \mathbf{C}_p' [p|\alpha] \right\} \otimes \mathbf{H}\boldsymbol{\Omega}\mathbf{H}' = \boldsymbol{\Psi} \otimes \mathbf{H}\boldsymbol{\Omega}\mathbf{H}', \quad (8)$$

186 where  $\boldsymbol{\Psi}$  is a matrix with  $(i, i')$  entries equal to the probabilities that species  $i$  shares a guild  
 187 with species  $i'$ . We term the  $\boldsymbol{\Psi}$  matrix to be the species proximity matrix due to the fact  
 188 that it forms a distance, of sorts, in the guild space of the species. Although, the covariance  
 189 is never negative between any two species, it can be zero, thus those species that occupy  
 190 different guilds will have uncorrelated  $\eta$  random effects, i.e., if  $\psi_{ii'} \approx 0$ , then  $\text{Cov}(\eta_{ij}, \eta_{i'j})$   
 191  $\approx 0$ .

192 It should be noted, however, that although the covariance of the  $\boldsymbol{\eta}$  random effect is  
 193 generally, positive, that does not mean that there are only ‘positive’ (or zero) relationships  
 194 between species. The clustering is based on the relationship each species has with the chosen  
 195 covariates. For example, one species may react positively along a covariate gradient ( $\delta_i > 0$ )  
 196 and another reacts negatively along that same gradient ( $\delta_i < 0$ ), therefore if a new site has  
 197 a high level of this covariate, the first species will be predicted to be relatively abundant,  
 198 while the other species prediction will be lower.

## 199 **2.2 Bayesian inference**

200 Because of the hierarchical and variable dimensional nature of the parameter space of the  
 201 DP-JSDM model we employ a Bayesian approach via MCMC (Markov Chain Monte Carlo)  
 202 for model fitting and inference. The posterior distribution of interest is given by

$$203 \quad [\mathbf{z}, p, \boldsymbol{\delta}_p, \boldsymbol{\beta}, \boldsymbol{\omega}, \boldsymbol{\sigma} | \mathbf{n}] \propto [\mathbf{n} | \mathbf{z}] [\mathbf{z} | \boldsymbol{\beta}, \boldsymbol{\delta}_p, \boldsymbol{\sigma}] \quad (9)$$

$$\times [\boldsymbol{\delta}_p | \boldsymbol{\omega}, p] [p | \alpha] [\boldsymbol{\omega}] [\boldsymbol{\sigma}] [\boldsymbol{\beta}] [\alpha],$$

204 where  $[\boldsymbol{\omega}]$ ,  $[\boldsymbol{\sigma}]$ ,  $[\boldsymbol{\beta}]$ , and  $[\alpha]$  are the prior distributions for the parameters.

205 There are several derived parameters which may be of interest for making desired eco-  
206 logical inference. First, are predictions of community abundance rates at new locations or  
207 times. Second, one may be interested in the overall effect of the environmental covariates for  
208 a particular species represented by  $\bar{\delta}_i$ . Finally, the matrix  $\mathbf{C}_p\mathbf{C}'_p$  is an  $I \times I$  indicator that a  
209 species is in the same guild (associated with) another species. The posterior mean of  $\mathbf{C}_p\mathbf{C}'_p$   
210 provides estimated guild proximity matrix,  $\Psi$ . Finally, the number of guilds,  $\kappa_p$  (number of  
211 columns in  $\mathbf{C}_p$ ) may be of interest.

212 The most direct way to make inferences on the proposed hierarchical clustering model is  
213 through a reversible-jump Markov chain Monte Carlo (RJMCMC) algorithm (Green, 2003)  
214 to sample the posterior distribution of the parameters and clustering assignment. Here, we  
215 provide an overview of the RJMCMC, additional details of the sampler are given in Appendix  
216 A.

217 In our description, we will assume the following prior distributions for the parameters:

$$\begin{aligned} 218 \quad [\boldsymbol{\beta}] &= \mathcal{N}(\boldsymbol{\mu}_\beta, \boldsymbol{\Sigma}_\beta), \quad [\boldsymbol{\delta}_p|\omega, p] = \mathcal{N}(\mathbf{0}, \mathbf{I}_{\kappa_p} \otimes \omega^2\mathbf{Q}), \\ 219 \quad [\omega] &= \mathcal{HT}(\phi_\omega, d_\omega), \quad [\sigma] = \mathcal{HT}(\phi_\sigma, d_\sigma) \\ 220 \quad [p|\alpha] &= \mathcal{CRP}(\alpha), \quad \text{and} \quad [\alpha] = \mathcal{G}(a, b), \end{aligned}$$

221 where  $\mathbf{I}_{\kappa_p}$  is an identity matrix of size  $\kappa_p$ ,  $\mathbf{Q}$  is a known positive-definite matrix,  $\mathcal{HT}(\phi, d)$   
222 represents a scaled half- $t$  distribution with scale parameter  $\phi$  and  $d$  degrees of freedom, and  
223  $\mathcal{G}$  represents a gamma distribution with parameters  $a$  and  $b$ . For most of these parameters,  
224 the priors can be adjusted to whatever distribution the user would like, the trade-off being a  
225 Metropolis-Hastings (MH) update instead of a Gibbs step (e.g., for  $\boldsymbol{\beta}$ ) or no difference at all  
226 if the parameter has to be updated with an MH step to begin with ( $\omega$ ,  $\sigma$ , and  $\alpha$ ). However,  
227 the normal  $[\boldsymbol{\delta}_p|\omega, p]$  prior is necessary to the proposed RJMCMC algorithm. Although, the  
228 known  $\mathbf{Q}$  is not necessary. This is not as critical as it sounds as the marginal distribution is

229 still a nonparametric DP process we just require that the base distribution be a multivariate  
230 normal.

231 The majority of the proposed RJMCMC algorithm is a standard Metropolis-within-Gibbs  
232 (hybrid) sampler for a GLM-like model (e.g., zero-inflated models might also be considered  
233 for the abundance distributions). Conditioned on a realization of  $p$ , all the other parameters  
234 can be updated with a traditional MH step or a Gibbs step. Hence, we do not focus on their  
235 updates here (see Appendix A). However, to update  $p$ , the dimension of the  $\delta_p$  vector will  
236 potentially change, necessitating the trans-dimensional aspect of the RJMCMC. Naively, the  
237 trans-dimensional moves require a joint  $(p, \delta_p)$  proposal which can be rejected often if one of  
238 those quantities is a bad fit for the current state of the remaining parameters even though the  
239 other is acceptable. Second, proposing new  $p$  such that the MCMC chain will mix well over  
240 the space of partitions is itself challenging. Because we are assuming that  $[\mathbf{z}|\beta, \delta_p, \sigma]$  and  
241  $[\delta_p|\omega, p]$  are multivariate normal, the first problem can be handled with the partial-analytic  
242 RJMCMC method proposed by Godsill (2001) and utilized by Johnson and Hoeting (2011)  
243 and Johnson et al. (2013b) in similar trans-dimensional MCMC applications. The partial-  
244 analytic method allows proposing new model ( $p$  in this case) without jointly proposing the  
245 associated model specific parameters ( $\delta_p$ ) because they can be analytically marginalized.  
246 This is a special case of a collapsed Gibbs sampler (Van Dyk and Park, 2008).

247 To produce efficient moves through cluster (guild) space we use the the “individual links”  
248 definition of the the CRP process proposed by Blei and Frazier (2011) and subsequently used  
249 by Johnson et al. (2013b) for clustering spatial abundance trends. The links version of the  
250 CRP process is constructed as follows:

- 251 1. A customer enters the restaurant and sits at one of an infinite number of tables.
- 252 2. The next customer enters and chooses to sit with the first customer with probability  
253  $1/(1 + \alpha)$  or a new table with probability  $\alpha/(1 + \alpha)$ .

254 3. In general, upon entering the restaurant, the  $i + 1$  customer sits with a previous *cus-*  
 255 *tom*er (not a table) with probability proportional to 1 or the new customer sit by  
 256 himself (self-links) with probability proportional to  $\alpha$ .

257 4. Groups are constructed by collecting all cliques of the mathematical graph formed by  
 258 the links between customers.

259 Blei and Frazier (2011) show that this definition of the CRP process is equivalent to the  
 260 traditional definition presented previously. However, MCMC sampling is now based on  
 261 sampling independent links between individuals. In terms of the multiple species model, let  
 262  $\ell_i \in \{1, \dots, i\}$  be the link for the  $i$ th species. The full conditional distribution of  $\ell_i$  is,

$$263 \quad [\ell_i | \cdot] \propto [\mathbf{z} | \boldsymbol{\beta}, \boldsymbol{\delta}_p, \boldsymbol{\sigma}] [\boldsymbol{\delta}_p | \omega, p] [\ell_i | \alpha], \quad (10)$$

264 where  $p$  is the partition constructed from all  $\ell_i$  and ,

$$265 \quad [\ell_i | \alpha] = \frac{\alpha 1_{\{\ell_i=i\}} + 1_{\{\ell_i < i\}}}{1 + \alpha}, \quad (11)$$

266 and  $1_{\{\cdot\}}$  is an indicator function for the condition in the brackets. It would be tempting to  
 267 sample from this discrete distribution in Gibbs fashion, however, note that it depends on  $\boldsymbol{\delta}_p$   
 268 which may be of different dimension under a different value of  $\ell_i$ . We can collapse over  $\boldsymbol{\delta}_p$   
 269 and use the marginal distribution

$$\begin{aligned} 270 \quad [\ell_i | \mathbf{z}, \boldsymbol{\beta}, \boldsymbol{\sigma}, \omega, \alpha] &= \int [\mathbf{z} | \boldsymbol{\beta}, \boldsymbol{\delta}_p, \boldsymbol{\sigma}] [\boldsymbol{\delta}_p | \omega, p] [\ell_i | \alpha] d\boldsymbol{\delta}_p \\ &= [\mathbf{z} | \boldsymbol{\beta}, \boldsymbol{\sigma}, \omega, p] [\ell_i | \alpha] \\ &\propto \mathcal{N}(\mathbf{z} | \mathbf{X}\boldsymbol{\beta}, \mathbf{K}_p(\mathbf{I}_{\kappa_p} \otimes \omega^2 \mathbf{Q})\mathbf{K}'_p + \boldsymbol{\Sigma}) [\ell_i | \alpha], \end{aligned} \quad (12)$$

271 which does not depend on  $\boldsymbol{\delta}_p$ . This approach was used by Johnson and Hoeting (2011) and  
 272 Johnson et al. (2013b), however, we found that for a large number of species and samples,  
 273 the covariance matrix  $\mathbf{K}_p(\mathbf{I}_{\kappa_p} \otimes \omega^2 \mathbf{Q})\mathbf{K}'_p + \boldsymbol{\Sigma}$  may be quite large and the inversion necessary

274 to evaluate the  $[\ell_i|\mathbf{z}, \boldsymbol{\beta}, \boldsymbol{\sigma}, \omega, \alpha]$  for each species and potential link would make the chain  
 275 prohibitively slow in practice. So, we sought an alternative formulation of the marginal  
 276 distribution that did not require inversion of such a large covariance matrix. Using Laplace’s  
 277 method (see Kass and Raftery 1995, Section 4.1) we can write

$$\begin{aligned} [\mathbf{z}|\boldsymbol{\beta}, \boldsymbol{\sigma}, \omega, p] &= \int [\mathbf{z}|\boldsymbol{\beta}, \boldsymbol{\delta}_p, \boldsymbol{\sigma}] [\boldsymbol{\delta}_p|\omega, p] d\boldsymbol{\delta}_p \\ &= (2\pi)^{\kappa_p/2} |\widehat{\mathbf{V}}_p|^{-1/2} \cdot \mathcal{N}(\widehat{\boldsymbol{\delta}}_p|\mathbf{0}, \mathbf{I}_{\kappa_p} \otimes \omega^2 \mathbf{Q}) \cdot \mathcal{N}(\mathbf{z}|\mathbf{X}\boldsymbol{\beta} + \mathbf{K}_p \widehat{\boldsymbol{\delta}}_p, \boldsymbol{\Sigma}), \end{aligned} \quad (13)$$

279 where  $\widehat{\mathbf{V}}_p = \mathbf{K}'_p \boldsymbol{\Sigma} \mathbf{K}_p + (\mathbf{I}_{\kappa_p} \otimes \omega^{-2} \mathbf{Q}^{-1})$  and  $\widehat{\boldsymbol{\delta}}_p = \mathbf{V}_p^{-1} (\mathbf{K}'_p \boldsymbol{\Sigma}^{-1} (\mathbf{z} - \mathbf{X}\boldsymbol{\beta}))$ , which are re-  
 280 spectively the inverse covariance and mean for the Gaussian full conditional distribution  
 281  $[\boldsymbol{\delta}_p|\mathbf{z}, \boldsymbol{\beta}, \boldsymbol{\sigma}, \omega, p]$ . This is the same distribution used to update  $\boldsymbol{\delta}_p$  with a Gibbs step following  
 282 an update of  $p$ . Normally, Laplace’s method produces an approximation to the integral, but  
 283 in this case the approximation is exact because the log integrand is quadratic in  $\boldsymbol{\delta}_p$  (Goutis  
 284 and Casella, 1999). By writing the integral in this way we need only invert  $\boldsymbol{\Sigma}$ , which is diag-  
 285 onal, and  $\mathbf{Q}$  because  $(\mathbf{I}_{\kappa_p} \otimes \omega^2 \mathbf{Q})^{-1} = \mathbf{I}_{\kappa_p} \otimes \omega^{-2} \mathbf{Q}^{-1}$ . If we use  $\mathbf{Q} = (\mathbf{H}'\mathbf{H})^{-1}$  as previously  
 286 suggested, then the inverse is trivial. Because,  $[\ell_i|\mathbf{z}, \boldsymbol{\beta}, \boldsymbol{\sigma}, \omega, \alpha]$  is relatively cheap to evalu-  
 287 ate for each  $\ell_i = 1, \dots, i$  we can use a Gibbs step and draw from the discrete distribution  
 288  $[\ell_i|\mathbf{z}, \boldsymbol{\beta}, \boldsymbol{\sigma}, \omega, \alpha]$  for each  $i = 1, \dots, I$ , with  $[\mathbf{z}|\boldsymbol{\beta}, \boldsymbol{\sigma}, \omega, p]$  evaluated using (13) instead of (12).

### 289 3 A Simulation Proof-of-Concept

290 To examine the ability of the CRP cluster model to make inference to species interaction, as  
 291 well as, to make joint community abundance predictions, we tested the model and RJMCMC  
 292 sampler with a small group of simulated data sets. In analyzing the simulated data our  
 293 objective was to assess whether the DP-JDSM model would, in practice, produce generally  
 294 correct estimates of the guild structure. Second, would the DP-JSDM exhibit the expected  
 295 behavior that as  $\omega$  becomes small, the number of guilds (groups) estimated will go to one as

296 the functional differences between the guilds (with respect to the variables in  $\mathbf{H}$ ) becomes  
297 insignificant.

### 298 3.1 Simulation and Analysis

299 Data were simulated for  $I = 20$  species,  $J = 35$  samples, and  $\kappa_p = 5$  groups. Six data sets  
300 were simulated corresponding to  $\omega$  equal to 0.25, 0.5, 0.75, 1, 1.5, and 2. While the true  
301 number of groups is always technically equal to five, the practical differences between the  
302 groups tends to zero as  $\omega$  becomes smaller. The group sizes were  $g_{pk} = 7, 5, 4, 3,$  and 1.  
303 Three environmental variables composing the guild design matrix  $\mathbf{H}$  were generated from a  
304 standard normal distribution. In addition, a single survey effort variable,  $\mathbf{x}$  was generated to  
305 adjust overall abundance measurement. The global design matrix was set to  $\mathbf{X} = [\mathbf{1}, \mathbf{x}, \mathbf{H}_x]$ ,  
306 where  $\mathbf{H}_x = [\mathbf{H}' | \dots | \mathbf{H}']'$ , that is,  $\mathbf{H}$  matrix is concatenated  $I$  times over species. Thus,  
307  $\boldsymbol{\delta}_p$  denotes guild differences from the overall global effect of the environmental variables,  
308  $\mathbf{H}$ . In order to maintain identifiability, we imposed the constraint that  $\sum_{k=1}^{\kappa_p} \boldsymbol{\delta}_k = \mathbf{0}$ . The  
309 global coefficient was set to  $\boldsymbol{\beta} = (2, 1, 0, -1, 0.5)'$  and each  $\boldsymbol{\delta}_k$ ;  $k = 1, \dots, 5$ , was drawn  
310 from  $N(\mathbf{0}, \omega^2 \mathbf{H}'\mathbf{H})$ . In these simulations all  $\sigma_{ij} = 0$ , therefore,  $\mathbf{z} \equiv \mathbf{X}\boldsymbol{\beta} + \mathbf{K}_p\boldsymbol{\delta}_p$ . However,  
311 a common  $\sigma$  was estimated in each analysis using a Poisson observation model, that is,  
312  $[n_{ij}|z_{ij}] = \text{Poisson}(e^{z_{ij}})$ .

313 The prior distributions used were the same as specified in Section 2.2, specifically,

- 314 •  $[\boldsymbol{\beta}]$ :  $\boldsymbol{\mu}_\beta = (\hat{\mu}_0, 0, 0, 0)'$  and  $\hat{\mu}_0$  is the log of the mean observed count and  $\boldsymbol{\Sigma}_\beta =$   
315  $100(\mathbf{X}'\mathbf{X})^{-1}$ .
- 316 •  $[\omega]$ :  $\phi_\omega = 1$  and  $d_\omega = 1$  which implies a half-Cauchy prior distribution.
- 317 •  $[\sigma]$ :  $\phi_\sigma = 1$  and  $d_\sigma \rightarrow \infty$  which implies a half-normal prior distribution.
- 318 •  $[\alpha]$ :  $a = 0.258$  and  $b = 0.038$ .

319 The prior distribution parameters for the gamma distribution  $[\alpha]$  were chosen based upon the  
320 method of Dorazio (2009) with one alteration. Dorazio (2009) used the method to choose  $a$   
321 and  $b$  such that the prior distribution over the number of groups was approximately uniform,  
322 that is,  $[\kappa_p] \approx 1/I$ ,  $\kappa_p = 1, \dots, I$ . However, we agree with the philosophy of Casella et al.  
323 (2014) that *a priori* we should prefer fewer groups, therefore, using the same optimization  
324 approach as Dorazio (2009), we chose  $a$  and  $b$  such that, approximately,  $[\kappa_p] \propto 1/\kappa_p$ . So, all  
325 else being equal, a smaller number of groups is *a priori* preferred.

326 For each of the six simulated datasets, we sampled the posterior distribution (9) using  
327 the RJMCMC algorithm detailed in Appendix A. Each sample consisted of 50,000 iterations  
328 following a burnin of 10,000 iterations. We created the `multAbund`<sup>2</sup> package for the R sta-  
329 tistical environment (R Development Core Team, 2015) which contains the code to run the  
330 RJMCMC algorithm described in Appendix A.

## 331 3.2 Simulation results

332 As expected, when  $\omega$  became small the DP-JSDM model was not able to distinguish guild  
333 differences between the species and essentially estimated one single group (Figure 1  $\omega =$   
334 0.25). As  $\omega$  increased and guild differences became apparent the model was able to separate  
335 the species into their respective guilds reasonably well (Figure 1). In addition, as  $\omega$  became  
336 large the precision with which the number of guilds was estimated increased as well (Figure  
337 2). There may be some bias as a few of the simulation runs produced  $\hat{\kappa}_p = 6$  (Figure 2;  
338  $\omega = 1$  and 2), however, a full simulation experiment would be necessary to assess that fact.

---

<sup>2</sup>Available from github at: <https://github.com/dsjohnson/multAbund>. The package can be installed from within an R session using the `devtools` package, but users need to be able to compile source code on their platform as the `multAbund` package uses C++ code in its routines.



## 339 4 Example: Mesopelagic fish abundance

### 340 4.1 Data

341 In our next demonstration of the DP-JSDM we analyze community structure and abundance  
342 of fishes that migrate diurnally between three mesopelagic depths in the eastern Bering Sea  
343 near Alaska. The tendency for most mesopelagic species to vertically migrate makes them an  
344 important trophic link between the deep scattering layer and upper surface waters (Sinclair  
345 et al., 2015) yet, fundamental aspects of multi-species distributions and relative abundances  
346 have not been previously described.

347 The field effort identified three primary sample stations over highly productive areas of  
348 the eastern Bering Sea pelagic (Figure 3). In the summers of 1999 and 2000 a total of 29  
349 daytime and 16 nighttime trawls were conducted at three depths (250, 500, and 1000 m)  
350 during a narrow sampling period. Four of these trawls were not analyzed due to technical  
351 difficulties in the field and we discarded them, resulting in  $J = 41$  samples. Trawls were run  
352 at-depth for 15–90 minutes resulting in collections of over 50,000 individuals representing 55  
353 species of fish and squid. Essentially, each individual trawl sample represents a community  
354 as influenced by depth and time of day. Here we will demonstrate the DP-JSDM using  
355  $I = 20$  of the relatively most common fish species (as opposed to squids, etc.).

356 The variables we put in the  $\mathbf{H}$  design matrix reflect the belief that the species segre-  
357 gate into guilds based on diurnal vertical migration characteristics. So, the guild covariates  
358 recorded for each trawl are daylight cycle (day or night) and depth category (250m, 500m,  
359 or 1000m). Here we used the full interaction model to define the  $\mathbf{H}$  design matrix (i.e., ‘ $\sim$   
360 `cycle*depth`’ in R language model syntax). Because the duration of the trawl varied from  
361 survey to survey, the duration was included in the  $\mathbf{X}$  matrix to model the overall abundance  
362 of fish caught in the trawl.

## 363 4.2 Model and analysis

364 Initial attempts at fitting a DP-JSDM proceeded in the same manner as the analysis of the  
365 simulation data in the previous section. Namely, we used the same Poisson model for the  
366 observed abundance counts. However, after initial fittings it became evident that the trawl  
367 data set possessed a significant level of zero-inflation relative to the Poisson distribution.  
368 This is likely due to the spatial patchiness of pelagic fish occurrence distributions (Benoit-  
369 Bird and Au, 2003). In addition, there may also be detection issues in the survey such that  
370 a zero count in the trawl does not necessarily mean absence of the species. However, unlike  
371 Dorazio and Connor (2014) we do not have replicated surveys in which to separate detection  
372 and absence. Therefore, we utilized a zero-inflated Poisson (ZIP) model in place of a Poisson  
373 GLM. The ZIP model used for this analysis is

$$374 \quad [n_{ij}|z_{ij}, \gamma_i] = \gamma_i 1_{[n_{ij}=0]} + (1 - \gamma_i) \text{Poisson}(n_{ij}|e^{z_{ij}}), \quad (14)$$

375 where  $1_{[n_{ij}=0]}$  is an indicator of a zero count and  $\gamma_i$  is a species-specific zero-inflation mixture

$$376 \quad [\text{logit } \gamma_i] = \mathcal{T}(\phi_\gamma, d_\gamma), \quad (15)$$

377 with scale parameter  $\phi_\gamma = 1.5$  and degrees of freedom  $d_\gamma = 6$ . This prior results in the  
378 translated prior for  $\gamma_i$  that is approximately uniform in (0,1). For the remaining parameters  
379 we used the same prior specification as the simulated data analysis of Section 3.1.

380 To assess if there is any improvement gained by using the DP-JSDM we also fitted the  
381 ‘independent species’ JSDM, that is  $\kappa_p = I$ , to the data. The JSDM we fitted was did not  
382 truly treat each species independently because there are shared terms in the  $\mathbf{X}$  design matrix  
383 (trawl duration) but it allows us to assess improvement in classifying animals into functional  
384 guilds relative to cycle and depth over treating them separately. To ascertain the magnitude  
385 of improvement we would have liked to be able to use the ‘leave one out’ Bayesian predictive

386 information criterion (BPIC) given by

$$\begin{aligned}
 -2 \text{ BPIC} &= -2 \sum_{i,j} E\{\log[n_{ij} | \mathbf{n}_{-(i,j)}, \mathbf{z}_{-(i,j)}, \boldsymbol{\gamma}, \boldsymbol{\beta}, \boldsymbol{\delta}_p, p, \boldsymbol{\sigma}, \omega, \alpha]\} \\
 &= -2 \sum_{i,j} E\{\log[n_{ij} | \mathbf{n}_{-(i,j)}, \mathbf{z}_{-(i,j)}, \boldsymbol{\gamma}]\}
 \end{aligned}
 \tag{16}$$

388 where  $\mathbf{n}_{-(i,j)}$  is a vector of all observed data except  $n_{ij}$  and  $\log[n_{ij} | \mathbf{n}_{-(i,j)}, \boldsymbol{\gamma}, \boldsymbol{\beta}, \boldsymbol{\delta}_p, p, \boldsymbol{\sigma}, \omega, \alpha]$   
 389 is the log posterior predictive density for the  $(i, j)$ th observation. However, it would be com-  
 390 putationally infeasible to rerun the RJMCMC for every left out  $(i, j)$  entry. So, we used the  
 391 ‘Widely Applicable Information Criterion’ (WAIC; Watanabe (2013)) as an approximation  
 392 (Watanabe, 2010; Link and Sauer, 2016) to  $-2$  BPIC, where

$$\begin{aligned}
 \text{WAIC} &= -2 \sum_{i,j} E\{\log[n_{ij} | \mathbf{n}, \mathbf{z}, \boldsymbol{\gamma}]\} \\
 &\quad + 2 \sum_{i,j} \text{Var}\{\log[n_{ij} | \mathbf{n}, \mathbf{z}, \boldsymbol{\gamma}]\}
 \end{aligned}
 \tag{17}$$

394 The WAIC requires only one run of the RJMCMC with the full data set. There are also  
 395 other selection methods applicable, see Hooten and Hobbs (2015) for others.

396 The model was fitted using the R package `multAbund`. The RJMCMC algorithm was run  
 397 for 100,000 iterations following a burnin of 10,000 iterations. The package contains code  
 398 to fit the Poisson abundance data model as well as the ZIP and Bernoulli probit model for  
 399 occurrence. In addition to the joint analysis of abundance, we also analyzed the trawl survey  
 400 data as an occurrence data set where  $y_{ij} = 1$  if  $n_{ij} > 0$ , else  $y_{ij} = 0$ .

### 401 4.3 Results

402 After fitting the ZIP version of the DP-JSDM and the independent species JSDM there was  
 403 a substantial improvement in WAIC under the DP-JSDM. WAIC for the DP-JSM model  
 404 was 3052.071 and WAIC = 3078.992 for the independence model. The posterior mode of the  
 405 number of guilds was  $\hat{\kappa}_p = 8$  with 95% of the posterior probability mass falling on  $\kappa_p = 8$

406 or 9 guilds. Figure 4 illustrates the estimated posterior matrix,  $\widehat{\Psi} = E[\mathbf{C}_p \mathbf{C}'_p]$  which defines  
407 the probability that any two species share the same vertical migration guild. Using  $1 - \widehat{\Psi}$   
408 as a measure of distance between species, we plotted the species according to the associated  
409 dendrogram (Figure 5), which gives a better visualization of the groupings. The predicted  
410 abundance for each species was calculated as  $\hat{\mathbf{n}}^* = E[\mathbf{n}^* | \mathbf{n}]$  where  $\mathbf{n}^* = (n_1^*, \dots, n_I^*)'$  is  
411 an observation under the observed environmental conditions (Figure 6). Results for the  $\gamma$   
412 parameters are presented in Table B.1 of Appendix B along with estimates of the  $\bar{\delta}_i$  values  
413 (Figure B.1). Appendix C provides similar figures and results for the DP-JSDM model using  
414 binary occurrence data instead of the observed abundance.

415 The model profiled a wide range in behavior among species from the two dominant  
416 fish families in the Bering Sea, Myctophidae and Bathylagidae. All but one of the 8 guilds  
417 described by the model (Figures 5 and C.2) include a single species from one or both of these  
418 families, implying that they partition the water column based on a characteristic response  
419 to physical factors and foraging requirements.

420 The accuracy and predictive capability of the model was confirmed by the correct clus-  
421 ter assignment of individual species with known relative abundance and depth distribution  
422 profiles in the Bering Sea (i.e., bathylagids, *Leuroglossus schmidti* and *Lipolagus ochotensis*).  
423 Then by virtue of guild membership, the model described distribution patterns in species for  
424 which there is little reported data (i.e., myctophids, *Stenobrachias leucopsarus* and *Diaphus*  
425 *theta*).

426 For instance, *L. schmidti* and *S. leucopsarus* formed the tightest cluster in both abundance  
427 and occurrence dendrograms (Figures 5 and C.2). Each is the most abundant species within  
428 their respective families in the Bering Sea (Brodeur et al., 1999; Sinclair et al., 1999) and  
429 both were highly represented throughout the water column day and night in this study.  
430 Guild identity with *L. schmidti* suggests that *S. leucopsarus* shares a similar life history and

431 foraging strategy wherein juveniles and adults have indistinct vertical migration and are  
432 stratified in the water column according to age (size) with adults remaining below 240 m  
433 (Beamish et al., 1999; Mecklenburg et al., 2002).

434 The bathylagid *L. ochotensis* and myctophid *D. theta* also form a guild in abundance  
435 (Figure 5) along with *Stenobrachias nannochir* in occurrence guilds (Figure C.2). *Lipolagus*  
436 *ochotensis* and *S. nannochir* are among the most abundant mesopelagic species in the Bering  
437 Sea Sinclair et al. (1999); Mecklenburg et al. (2002). Both are size-stratified by depth with  
438 adults residing in the deepest layers and especially present between 500-1000 m (Mecklenburg  
439 et al., 2002). As a strong vertical migrator, *L. ochotensis* is also abundant between 200-500  
440 m Sinclair et al. (1999); Mecklenburg et al. (2002). Little is known about *D. theta* from  
441 directed catch in the Bering Sea, however guild identity with *S. nannochir* and especially  
442 with *L. ochotensis* suggests they share similar patterns of behavior. The model implication  
443 that *D. theta* is an age-stratified strong vertical migrator available at upper mesopelagic  
444 depths (Figure 6, B.1, and C.3) is supported by observations that it is a primary prey item  
445 of Dall's porpoise (*Phocoenoides dalli*) in the top 250 m of water column (Crawford, 1981).

446 The best example of the degree of fine detail captured by the model was demonstrated by  
447 *Bathylagus pacificus*, a common and abundant species of Bathylagidae that formed its own  
448 cluster (Figure 5). Like other members of its family *B. pacificus* demonstrates a bimodal  
449 pattern in body size at depth (Peden et al., 1985; Mecklenburg et al., 2002). In our study,  
450 juvenile fish were concentrated at mid-layer levels during the day (500 meters) rising to 250  
451 meters at night, while adults concentrate at deeper daytime layers (1000 m) rising to 500  
452 m at night (Sinclair and Stabeno, 2002). This vertical migratory movement is apparent in  
453 the log abundance plots (Figure 6; and  $\bar{\delta}_i$  values in Figure B.1) that together with known  
454 age distribution suggest *B. pacificus* may form its own guild based on abundances at depth  
455 driven by varying foraging requirements of juvenile and adults.

## 456 5 Discussion

457 We presented a new methodology for modeling joint species distributions based on Dirichlet  
458 process random effects to model species associations through a latent guild structure. Instead  
459 of trying to directly parameterize cross-correlation in a species-specific random effect, we used  
460 latent membership in an ecological guild. Species belonging to the same guild followed the  
461 same response to environmental conditions through random coefficients effects in a GLM-like  
462 setting. Unlike simple cross-correlated species random intercepts, the DP-JSDM provides  
463 some valuable information on which species belong to guilds together and for the species  
464 within a guild, how they respond to the selected environmental conditions together.

465 A fundamental aspect of mesopelagic ecology is diel vertical migration. The DP-JSDM  
466 successfully identified community structure among 20 species of fish from the eastern Bering  
467 Sea within this framework. The selected model parameters of depth and light describe real-  
468 time clusters of species that move together similarly through the water column on a 24 hour  
469 cycle, presumably in relation to foraging. Based on studies conducted in the North Pacific  
470 Ocean, the diets of many of these same species collected from different depths match vertical  
471 distribution patterns of the variety of copepods and euphausiids that they consume (Beamish  
472 et al., 1999).

473 Although the DP-JSDM model was initially desired to model species association, it has  
474 the added benefit that it automatically adjusts to the necessary complexity because the  
475 number of guilds is also simultaneously being estimated as well. In the simulation experiment  
476 it was demonstrated that if there is apparently little difference between the species in their  
477 response to the recorded environmental conditions the DP-JSDM will collapse to one guild,  
478 that is, no statistical difference between the species. This reduction in model complexity  
479 was noted by Johnson et al. (2013b) in reference to spatially clustering abundance trends.

480 In our description of the model and our examples, we have provided a relatively straight-

481 forward demonstration of the model and associated RJMCMC algorithm. However, there  
482 are several extensions that would be useful in other ecological settings. Here we did not  
483 have repeated observations at each site, so, we could not add an identifiable detection model  
484 to the observation process, although, we illustrated that covariates (i.e., trawl duration)  
485 could be added as a quasi-detection model as Ver Hoef and Frost (2003) used. However, if  
486 multiple observations are available for each site, then a detection process could be added to  
487 the observation model. Dorazio and Connor (2014) made use of an  $N$ -mixture model and  
488 the DP-JSDM could use that as well. Instead of the ZIP model, one could add a another  
489 observation model,

$$490 \quad [\tilde{n}_{ijk}, n_{ij} | \dots] = \text{Binomial}(\tilde{n}_{ijk} | n_{ij}, \gamma_{ijk}) \text{Poisson}(n_{ij} | z_{ij}), \quad (18)$$

491 as the observation portion of the model, where  $\tilde{n}_{ij}$  is the observed abundance of species  $i$  at  
492 site  $j$  during survey  $k$  and  $\gamma_{ijk}$  is the probability of each of the  $n_{ij}$  individuals being observed.  
493 If one marginalizes over the true abundances, the Poisson observation model results,

$$494 \quad [\tilde{n}_{ijk} | \gamma_{ijk}, z_{ij}] = \text{Poisson}(\tilde{n}_{ijk} | \log \gamma_{ijk} + z_{ij}), \quad (19)$$

495 where  $E[n_{ijk}] = \exp\{\log \gamma_{ijk} + z_{ij}\}$ . The same approach could also be used for occurrence  
496 modeling, in which case, it becomes occupancy modeling, that is, for the observed presence  
497  $\tilde{y}_{ijk}$ , we use the hierarchical observation model,

$$498 \quad [\tilde{y}_{ijk}, y_{ij} | \dots] = \text{Bernoulli}(\tilde{y}_{ijk} | y_{ij} \gamma_{ijk}) \text{Bernoulli}(y_{ij} | z_{ij}), \quad (20)$$

499 where the probability that  $\tilde{y}_{ijk} = 1$  is  $y_{ij} \gamma_{ijk}$ . The main point being that the process model  
500 does not change in either of these two settings, so, the DP-JSDM can easily be adapted to  
501 these situations.

502 There is also an alteration that can be made when many sites are visited and spatial  
503 correlation between sights might also be a consideration. We are not calling this an extension,

504 because spatial correlation can be added without making additions to the basic structure  
505 presented. All that needs to be changed to add random spatial effects is to use the basis  
506 function approach of Ver Hoef and Jansen (2014), Johnson et al. (2013a), or Hefley et al.  
507 (2016). In under a spatial basis function model, the random spatial field is modeled as  $\boldsymbol{\eta} =$   
508  $\mathbf{H}\boldsymbol{\delta}$  where the columns of the matrix  $\mathbf{H}$  contain the spatial basis functions evaluated at each of  
509 the modeled sites (rows). Each basis column represents a different frequency. In the notation  
510 just presented it should be fairly obvious how the DP-JSDM can be changed to contain spatial  
511 correlation, one simply needs to use a basis function matrix for the environmental design  
512 matrix. In that case, it might be appropriate to use  $[\boldsymbol{\delta}|\omega] = \mathcal{N}(\mathbf{0}, \omega^2\mathbf{I})$  for the DP baseline  
513 distribution to match prior specifications that are usually used in spatial analysis. And, of  
514 course, one could combine the spatial model with the previously mentioned detection model  
515 extensions to form multivariate spatial models for occupancy and abundance modeling.

## 516 Acknowledgments

517 The findings and conclusions in the paper are those of the authors and do not necessarily  
518 represent the views of the National Marine Fisheries Service, NOAA. Reference to trade  
519 names does not imply endorsement by the National Marine Fisheries Service, NOAA.

## 520 References

- 521 Albert, J. and Chib, S. (1993). Bayesian-analysis of binary and polychotomous reponse data.  
522 *Journal of the American Statistical Association*, 88(422):669–679.
- 523 Beamish, R., Leask, K., Ivanov, O., Balanov, A., Orlov, A., and Sinclair, B. (1999). The



- 524 ecology, distribution, and abundance of midwater fishes of the subarctic pacific gyres.  
525 *Progress in Oceanography*, 43(2):399–442.
- 526 Benoit-Bird, K. J. and Au, W. W. (2003). Spatial dynamics of a nearshore, micronekton  
527 sound-scattering layer. *ICES Journal of Marine Science: Journal du Conseil*, 60(4):899–  
528 913.
- 529 Blei, D. M. and Frazier, P. I. (2011). Distance dependent chinese restaurant processes.  
530 *Journal of Machine Learning Research*, 12:2461–2488.
- 531 Brodeur, R. D., Wilson, M. T., Walters, G. E., and Melnikov, I. V. (1999). Forage fishes  
532 in the bering sea: distribution, species associations, and biomass trends. *Dynamics of the*  
533 *Bering Sea*, pages 509–536.
- 534 Carroll, C., Johnson, D. S., Dunk, J. R., and Zielinski, W. J. (2010). Hierarchical bayesian  
535 spatial models for multispecies conservation planning and monitoring. *Conservation Bi-*  
536 *ology*, 24(6):1538–1548.
- 537 Casella, G., Moreno, E., and Girón, F. J. (2014). Cluster analysis, model selection, and prior  
538 distributions on models. *Bayesian Analysis*, 9:613–658.
- 539 Clark, J. S., Gelfand, A. E., Woodall, C. W., and Zhu, K. (2014). More than the sum  
540 of the parts: forest climate response from joint species distribution models. *Ecological*  
541 *Applications*, 24(5):990–999.
- 542 Crawford, T. W. (1981). Vertebrate prey of phocoenoides dalli,(dall’s porpoise): associated  
543 with the japanese high seas salmon fishery in the north pacific ocean. Master’s thesis,  
544 University of Washington.

- 545 Cressie, N., Calder, C. A., Clark, J. S., Hoef, J. M. V., and Wikle, C. K. (2009). Account-  
546 ing for uncertainty in ecological analysis: the strengths and limitations of hierarchical  
547 statistical modeling. *Ecological Applications*, 19(3):553–570.
- 548 Dorazio, R. M. (2009). On selecting a prior for the precision parameter of dirichlet process  
549 mixture models. *Journal of Statistical Planning and Inference*, 139(9):3384–3390.
- 550 Dorazio, R. M. and Connor, E. F. (2014). Estimating abundances of interacting species  
551 using morphological traits, foraging guilds, and habitat. *PloS one*, 9(4):e94323.
- 552 Dorazio, R. M., Mukherjee, B., Zhang, L., Ghosh, M., Jelks, H. L., and Jordan, F. (2008).  
553 Modeling unobserved sources of heterogeneity in animal abundance using a dirichlet pro-  
554 cess prior. *Biometrics*, 64(2):635–644.
- 555 Dunson, D. B. and Xing, C. (2009). Nonparametric bayes modeling of multivariate categor-  
556 ical data. *Journal of the American Statistical Association*, 104(487):1042–1051.
- 557 Godsill, S. (2001). On the relationship between Markov Chain Monte Carlo methods for  
558 model uncertainty. *Journal of Computational and Graphical Statistics*, 10:230–248.
- 559 Goutis, C. and Casella, G. (1999). Explaining the saddlepoint approximation. *The American*  
560 *Statistician*, 53(3):216–224.
- 561 Green, P. J. (2003). Trans-dimensional markov chain monte carlo. In Green, P. J., Hjort,  
562 N. L., and Richardson, S., editors, *Highly Structured Stochastic Systems*. Oxford University  
563 Press, Inc., New York.
- 564 Hefley, T. J., Broms, K. M., Brost, B. M., Buderman, F. E., Kay, S. L., Scharf, H. R.,  
565 Tipton, J. R., Williams, P. J., and Hooten, M. B. (2016). The basis function approach for  
566 modeling autocorrelation in ecological data. *Ecography*, In press.

- 567 Hobbs, N. T. and Hooten, M. B. (2015). *Bayesian models: a statistical primer for ecologists*.  
568 Princeton University Press.
- 569 Hooten, M. B. and Hobbs, N. T. (2015). A guide to Bayesian model selection for ecologists.  
570 *Ecological Monographs*, 85(1):3–28.
- 571 Johnson, D. S., Conn, P. B., Hooten, M. B., Ray, J. C., and Pond, B. A. (2013a). Spatial  
572 occupancy models for large data sets. *Ecology*, 94(4):801–808.
- 573 Johnson, D. S. and Fritz, L. (2014). agtrend: A bayesian approach for estimating trends of  
574 aggregated abundance. *Methods in Ecology and Evolution*, 5:1110–1115.
- 575 Johnson, D. S. and Hoeting, J. A. (2011). Bayesian multimodel inference for geostatistical  
576 regression models. *Plos One*, 6(11):e25677.
- 577 Johnson, D. S., Ream, R. R., Towell, R. G., Williams, M. T., and Guerrero, J. D. L. (2013b).  
578 Bayesian clustering of animal abundance trends for inference and dimension reduction.  
579 *Journal of Agricultural Biological and Environmental Statistics*, 18(3):299–313.
- 580 Kass, R. E. and Raftery, A. E. (1995). Bayes factors. *Journal of the American Statistical*  
581 *Association*, 90:773–795.
- 582 Latimer, A., Banerjee, S., Sang Jr, H., Mosher, E., and Silander Jr, J. (2009). Hierarchical  
583 models facilitate spatial analysis of large data sets: a case study on invasive plant species  
584 in the northeastern united states. *Ecology Letters*, 12(2):144–154.
- 585 Link, W. A. and Sauer, J. R. (2016). Bayesian cross-validation for model evaluation and  
586 selection, with application to the north american breeding survey. *Ecology*, In press.
- 587 McLachlan, G. and Peel, D. (2004). *Finite mixture models*. John Wiley & Sons.
- 588 Mecklenburg, C. W., Mecklenburg, T. A., and Thorsteinson, L. K. (2002). *Fishes of Alaska*.

- 589 Neal, R. (2000). Markov chain sampling methods for Dirichlet process mixture models.  
590 *Journal of Computational and Graphical Statistics*, 9(2):249–265.
- 591 Peden, A. E., Ostermann, W., and Pozar, L. J. (1985). *Fishes observed at Canadian Weath-*  
592 *ership Station Papa (500N, 1450W): with notes on the transpacific cruise of the CSS*  
593 *Endeavor*. Number 18. British Columbia Provincial Museum.
- 594 R Development Core Team (2015). *R: A Language and Environment for Statistical Com-*  
595 *puting*. R Foundation for Statistical Computing, Vienna, Austria.
- 596 Royle, J. A. (2004). N-mixture models for estimating population size from spatially replicated  
597 counts. *Biometrics*, 60(1):108–115.
- 598 Royle, J. A. and Dorazio, R. M. (2008). *Hierarchical Modeling and Inference in Ecology*.  
599 Academic Press- Elsevier Ltd.
- 600 Shaby, B. and Wells, M. T. (2011). Exploring an adaptive metropolis algorithm. Technical  
601 Report 2011-14, Department of Statistical Science, Duke University.
- 602 Simberloff, D. and Dayan, T. (1991). The guild concept and the structure of ecological  
603 communities. *Annual review of ecology and systematics*, pages 115–143.
- 604 Sinclair, E., Balanov, A., Kubodera, T., Radchenko, V., and Fedorets, Y. A. (1999). Dis-  
605 tribution and ecology of mesopelagic fishes and cephalopods. *Dynamics of the Bering*  
606 *Sea (TR Loughlin and K Ohtani, eds.)*, Alaska Sea Grant College Program AK-SG-99-03,  
607 *University of Alaska Fairbanks*, pages 485–508.
- 608 Sinclair, E. and Stabeno, P. (2002). Mesopelagic nekton and associated physics of the  
609 southeastern bering sea. *Deep Sea Research Part II: Topical Studies in Oceanography*,  
610 49(26):6127–6145.

- 611 Sinclair, E., Walker, W., and Thomason, J. (2015). Body size regression formulae, proximate  
612 composition and energy density of eastern Bering Sea mesopelagic fish and squid. *PloS*  
613 *ONE*, In press.
- 614 Thorson, J. T., Scheuerell, M. D., Shelton, A. O., See, K. E., Skaug, H. J., and Kristensen,  
615 K. (2015). Spatial factor analysis: a new tool for estimating joint species distributions  
616 and correlations in species range. *Methods in Ecology and Evolution*.
- 617 Tiao, G. C. and Zellner, A. (1964). Bayes's theorem and the use of prior knowledge in  
618 regression analysis. *Biometrika*, pages 219–230.
- 619 Van Dyk, D. A. and Park, T. (2008). Partially collapsed gibbs samplers: Theory and  
620 methods. *Journal of the American Statistical Association*, 103(482):790–796.
- 621 Ver Hoef, J. M. and Frost, K. J. (2003). A Bayesian hierarchical model for monitoring harbor  
622 seal changes in Prince William Sound, Alaska. *Environmental and Ecological Statistics*,  
623 10:201–219.
- 624 Ver Hoef, J. M. and Jansen, J. K. (2014). Estimating abundance from counts in  
625 large data sets of irregularly-spaced plots using spatial basis functions. *arXiv preprint*  
626 *arXiv:1410.3163*.
- 627 Vermunt, J. K., Van Ginkel, J. R., Der Ark, V., Andries, L., and Sijtsma, K. (2008). Mul-  
628 tiple imputation of incomplete categorical data using latent class analysis. *Sociological*  
629 *Methodology*, 38(1):369–397.
- 630 Ward, E. J., Chirakkal, H., Gonzalez-Suarez, M., Auriolles-Gamboa, D., Holmes, E. E., and  
631 Gerber, L. (2010). Inferring spatial structure from time-series data: using multivariate  
632 state-space models to detect metapopulation structure of california sea lions in the gulf of  
633 california, mexico. *Journal of Applied Ecology*, 47(1):47–56.

634 Watanabe, S. (2010). Asymptotic equivalence of bayes cross validation and widely applica-  
635 ble information criterion in singular learning theory. *The Journal of Machine Learning*  
636 *Research*, 11:3571–3594.

637 Watanabe, S. (2013). A widely applicable bayesian information criterion. *The Journal of*  
638 *Machine Learning Research*, 14(1):867–897.

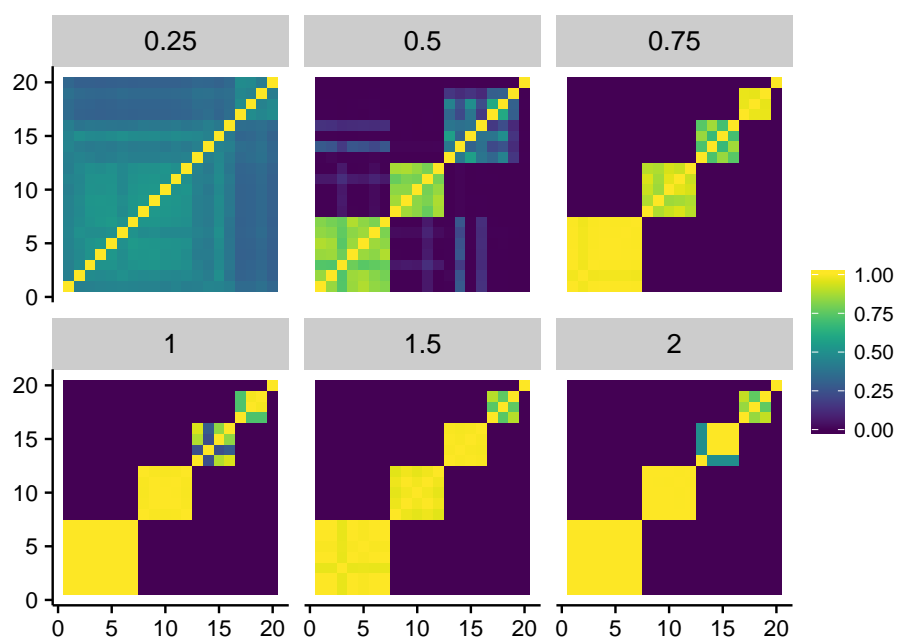


Figure 1: Estimated probabilities of joint guild membership between each species.

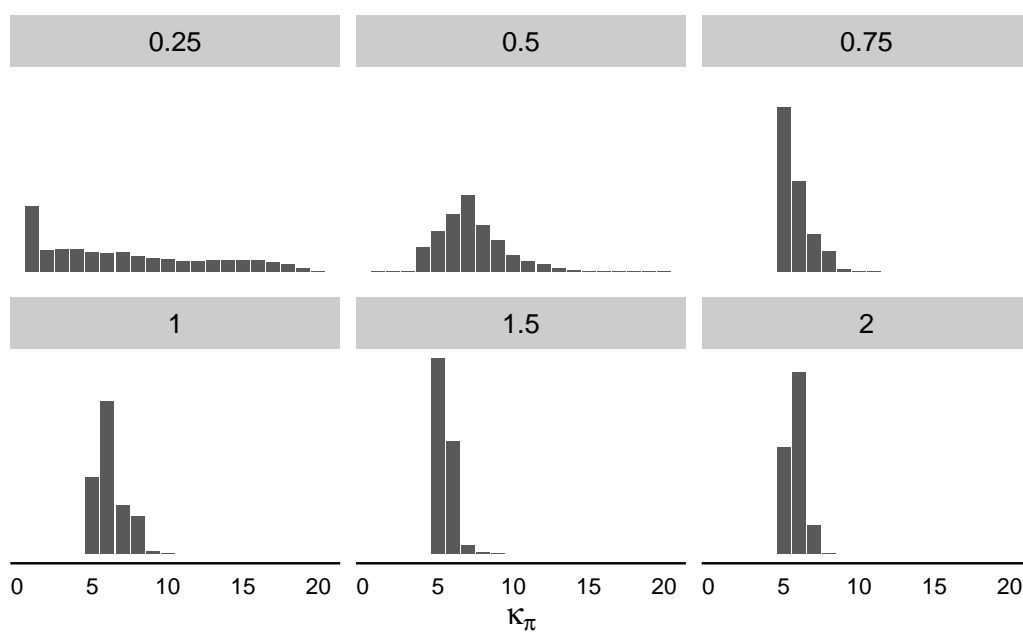


Figure 2: Estimated number of guilds,  $\kappa_p$ , for simulated Poisson data sets with  $\omega$  ranging from 0.25 to 2.



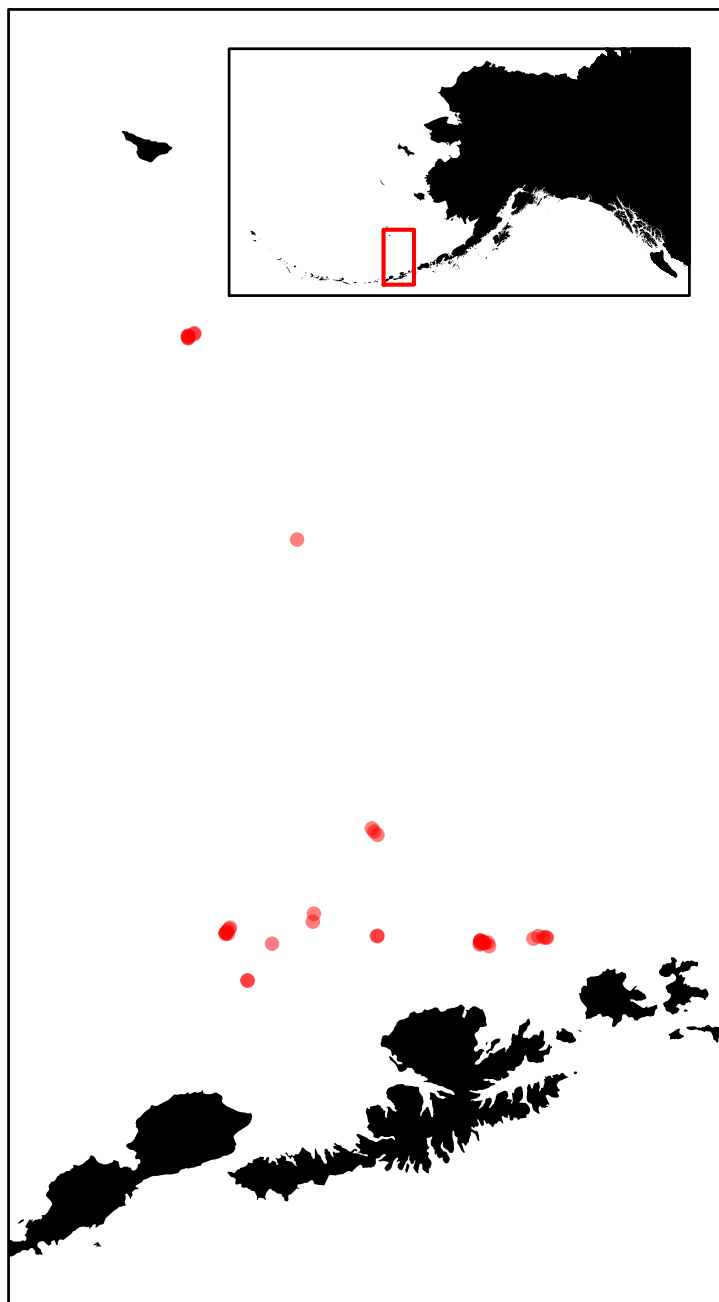


Figure 3: Locations of the mesopelagic trawl surveys. There were  $J = 41$  separate trawl surveys used the analysis of Section 4, however, some surveys were attempted geographically near other surveys, so, they are somewhat obscured in the figure.

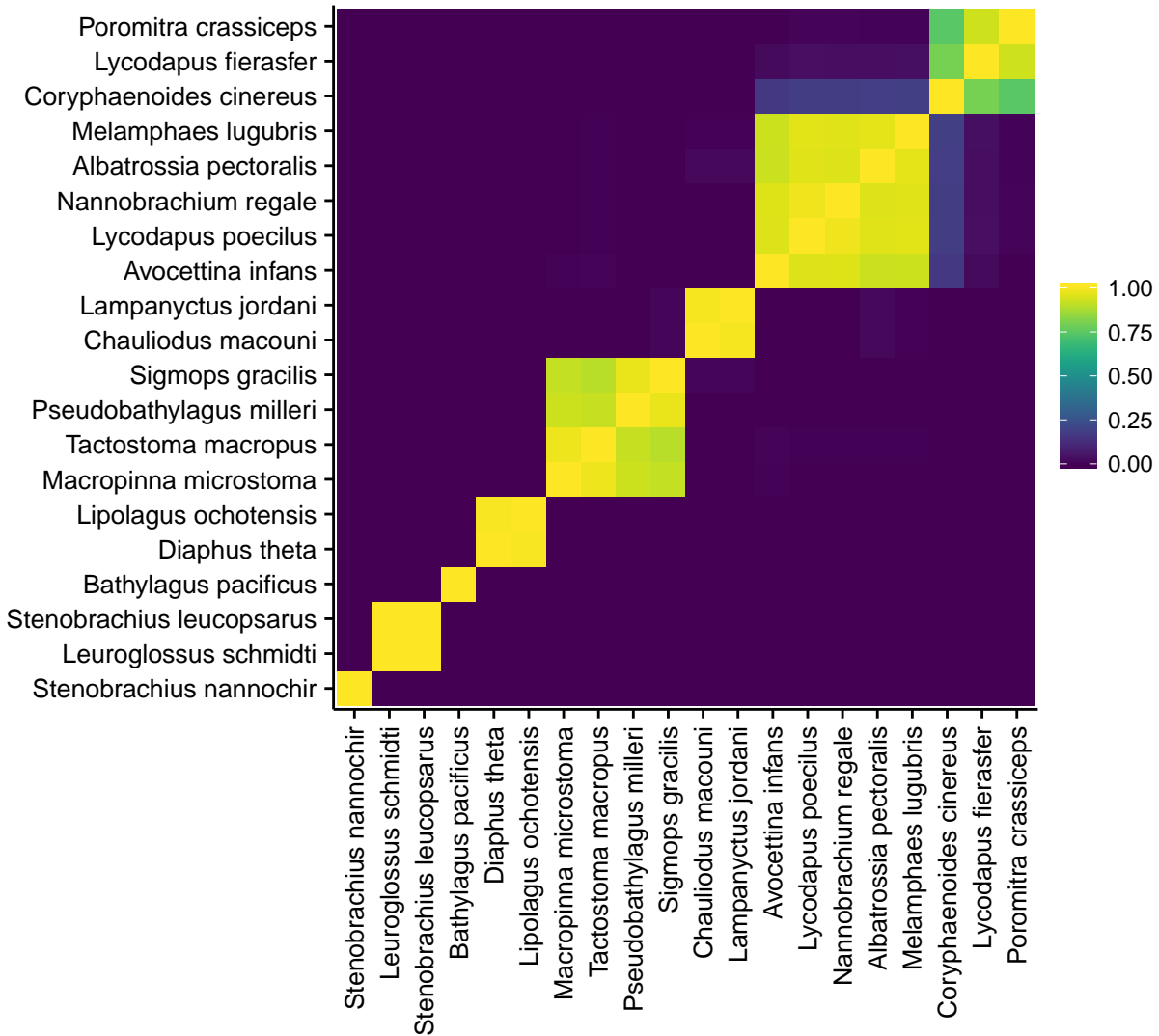


Figure 4: Estimated probability of joint guild membership for each of the fish species in the trawl survey with respect to abundance

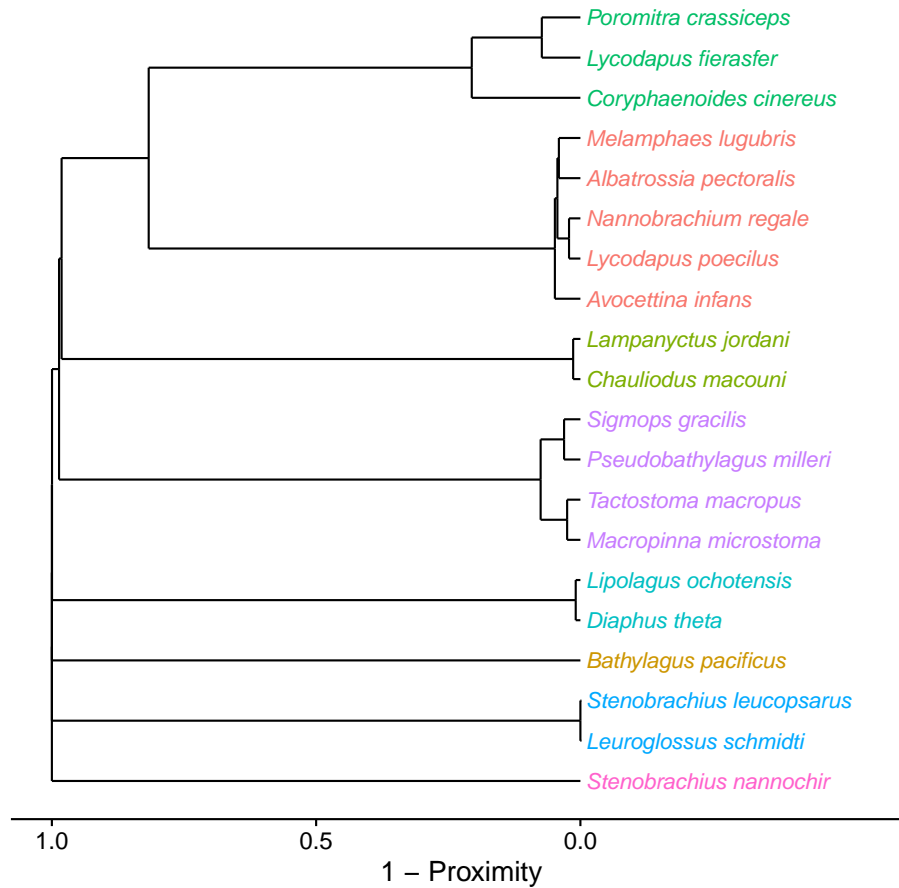


Figure 5: Clustering of trawl survey fish species based on the estimated probability of joint guild membership. The matrix  $1 - \hat{\Psi}$  was used as a distance matrix for forming the dendrogram. The colored labels reflect guild groupings based on the posterior mode number of guilds,  $\hat{\kappa}_p = 8$

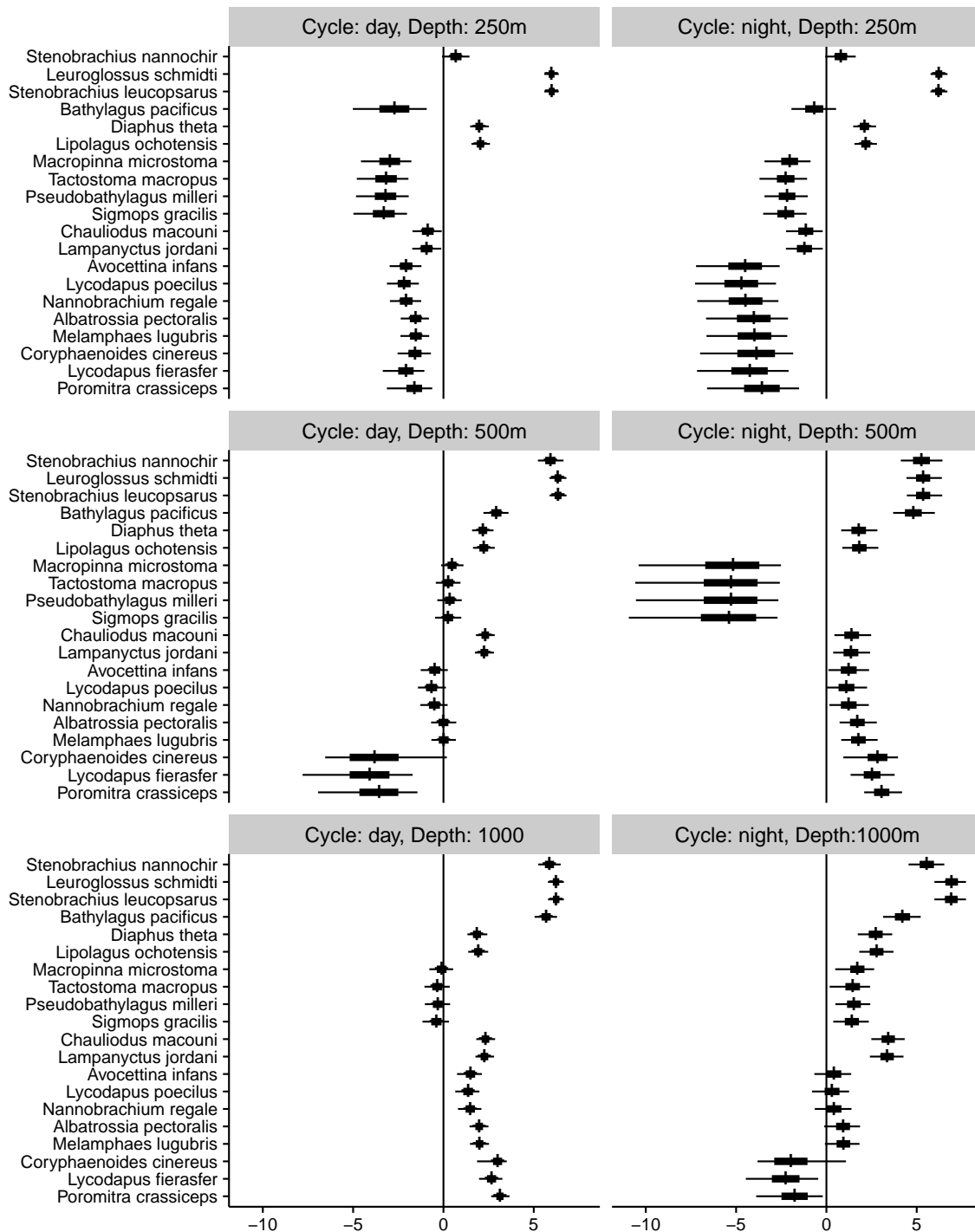


Figure 6: Species-specific predictions of log-abundance for each level of cycle (day or night), and depth (250, 500, or 1000 m).

## 639 Appendix A: RJMCMC details

### 640 A.1 Prior distributions

641 Here we describe the details for performing the necessary parameter updates in the RJMCMC  
642 algorithm. To facilitate the description the reader should recall we use the following prior  
643 distributions in full vector form (where appropriate):

644 •  $[\text{logit } \gamma_i] = \mathcal{T}(\phi_\gamma, d_\gamma)$  for  $i = 1, \dots, I$

645 •  $[\boldsymbol{\beta}] = \mathcal{N}(\boldsymbol{\mu}_\beta, \boldsymbol{\Sigma}_\beta)$ ,

646 •  $[\boldsymbol{\delta}_p | \boldsymbol{\omega}] = \mathcal{N}(\mathbf{0}, \mathbf{I}_{\kappa_p} \otimes \boldsymbol{\omega}^2(\mathbf{H}'\mathbf{H})^{-1})$ ,

647 •  $[\boldsymbol{\omega}] = \mathcal{HT}(\phi_\omega, d_\omega)$

648 •  $[\sigma] = \mathcal{HT}(\phi_\sigma, d_\sigma)$

649 •  $[p | \alpha] = \mathcal{CRP}(\alpha)$

650 •  $[\alpha] = \mathcal{G}(a, b)$ ,

651 where  $\mathcal{T}$  denotes a  $t$  distribution,  $\mathcal{N}$  is a (multivariate) normal distribution,  $\mathcal{HT}$  is a half- $t$   
652 distribution,  $\mathcal{CRP}$  is the Chinese restaurant process, and  $\mathcal{G}$  is a gamma distribution. Now, we  
653 can describe the Markov Chain Monte Carlo (MCMC) sampler. The sampler is constructed  
654 from repeated draws from the full conditional posterior distributions. We use the notation  
655  $[x | \cdot]$  to represent the conditional distribution of the variable ‘ $x$ ’ given all of the other model  
656 components.

### 657 A.2 Updating $\mathbf{z}$

658 We will first describe the updating of  $\mathbf{z}$  for the abundance models. Unfortunately, for the  
659 abundance models used in this paper (e.g.,  $[n_{ij} | z_{ij}, \boldsymbol{\gamma}] = \text{ZIP or Poisson}$ ), the full conditional

660 distribution does not exist in a nice closed form and we suspect this is the case for every  
 661 abundance model one may want to use. The full conditional distribution required for the  
 662 update is,

$$663 \quad [\mathbf{z}|\cdot] \propto [\mathbf{n}|\mathbf{z}, \gamma] \cdot \mathcal{N}(\mathbf{z}|\mathbf{X}\boldsymbol{\beta} + \mathbf{K}_p\boldsymbol{\delta}_p, \boldsymbol{\Sigma}), \quad (\text{A.1})$$

664 for which a Metropolis-Hastings (MH) step is used with a random walk proposal distribution  
 665  $[\mathbf{z}^*|\mathbf{z}] = N(\mathbf{z}, \mathbf{R}_z)$ , where  $\mathbf{R}_z$  is a diagonal matrix that is tuned for optimal sampling. In  
 666 the R package `multAbund` we use the adaptive random walk proposal described by Shaby  
 667 and Wells (2011) that continually adjusts proposal distribution throughout the MCMC run.  
 668 Once the new  $\mathbf{z}^*$  is drawn, each  $z_{ij}^*$  is accepted with probability

$$669 \quad \max \left\{ 1, \frac{[z_{ij}^*|\cdot]}{[z_{ij}|\cdot]} \right\}. \quad (\text{A.2})$$

670 Note, that even though  $\mathbf{z}^*$  is proposed as a vector, the independence of each element implies  
 671 that each  $z_{ij}^*$  can be accepted or rejected independently.

672 If one is analyzing occurrence data with a probit link as described in the main text of  
 673 the paper, then the full conditional distribution,

$$674 \quad [\mathbf{z}|\cdot] \propto [\mathbf{y}|\mathbf{z}] \cdot \mathcal{N}(\mathbf{z}|\mathbf{X}\boldsymbol{\beta} + \mathbf{K}_p\boldsymbol{\delta}_p, \boldsymbol{\Sigma}), \quad (\text{A.3})$$

675 is available in closed form. For each  $(i, j)$ , the necessary full conditional distribution is

$$676 \quad [z_{ij}|\cdot] = \mathcal{N}_{a_{ij}}^{b_{ij}}(\mathbf{X}\boldsymbol{\beta} + \mathbf{K}_p\boldsymbol{\delta}_p, \boldsymbol{\Sigma}), \quad (\text{A.4})$$

677 where  $\mathcal{N}_{a_{ij}}^{b_{ij}}$  is a truncated normal distribution with lower bound

$$678 \quad a_{ij} = \begin{cases} -\infty & \text{for } y_{ij} = 0 \\ 0 & \text{for } y_{ij} = 1 \end{cases} \quad (\text{A.5})$$

679 and upper bound

$$680 \quad b_{ij} = \begin{cases} 0 & \text{for } y_{ij} = 0 \\ \infty & \text{for } y_{ij} = 1 \end{cases} \quad (\text{A.6})$$

681 (Albert and Chib, 1993). If another link function is used, then the same procedure as the  
 682 abundance model updates is used with a MH acceptance step.

### 683 A.3 Updating $\gamma$

684 Here, the only model used where  $\gamma$  was present is the ZIP model used in the analysis of the  
 685 fish survey data. Therefore, we only describe updating of this parameter with respect to the  
 686 ZIP model with species-specific ZIP parameters,  $\gamma_i$ . The full conditional distribution of logit  
 687  $\gamma_i$  is

$$688 \quad [\text{logit } \gamma_i | \cdot] = [\mathbf{n}_i | \mathbf{z}_i, \gamma_i] \cdot \mathcal{T}(\text{logit } \gamma_i | \phi_\gamma, d_\gamma). \quad (\text{A.7})$$

689 As with the  $\mathbf{z}$  updates, the adaptive random walk MH update  $\mathcal{N}(\{\text{logit } \gamma_i, R_\gamma\})$  was used  
 690 where  $R_\gamma$  is continually adapted through the RJMCMC.

### 691 A.4 Updating $\beta$ and $\delta_p$

692 All of the coefficient vectors in the model have a normal prior distribution, thus the full  
 693 conditional distributions  $[\beta | \cdot]$  and  $[\delta_p | \cdot]$  are normal distributions where each is given in  
 Table A.1.

Table A.1: Means and variances for sampling of  $\beta$  and  $\delta_p$ . Each parameter has a full conditional distribution of the form  $\mathcal{N}(\mathbf{V}^{-1}\mathbf{m}, \mathbf{V}^{-1})$ .

Distribution	$\mathbf{V}$	$\mathbf{m}$
$[\beta   \cdot]$	$\mathbf{X}'\Sigma^{-1}\mathbf{X} + \Sigma_\beta^{-1}$	$\mathbf{X}'\Sigma^{-1}(\mathbf{z} - \mathbf{K}\delta_p) + \Sigma_\beta^{-1}\boldsymbol{\mu}_\beta$
$[\delta_p   \cdot]$	$\mathbf{K}'_p\Sigma^{-1}\mathbf{K}_p + (\mathbf{I}_{\kappa_p} \otimes \Omega)^{-1}$	$\mathbf{K}'_p\Sigma^{-1}(\mathbf{z} - \mathbf{X}\beta)$

694

## 695 **A.5 Updating $\omega$ and $\sigma$**

696 Using an  $\mathcal{HT}$  family of priors is not directly conjugate, therefore, a MH step is used here as  
 697 well. Recall that here we are using  $\mathbf{\Omega} = \omega^2(\mathbf{H}'\mathbf{H})^{-1}$  and  $\mathbf{\Sigma} = \sigma^2\mathbf{I}$ , where  $\omega = \exp(\xi)$  and  
 698  $\sigma = \exp(\theta)$ . These choices could be easily modified if desired. For  $\omega$ , the full conditional  
 699 distribution is given by

$$700 \quad [\omega|\cdot] \propto \mathcal{N}(\boldsymbol{\delta}_p|\mathbf{0}, \mathbf{I}_{\kappa_p} \otimes \mathbf{\Omega}) \cdot \mathcal{HT}(\omega|\phi_\omega, d_\omega). \quad (\text{A.8})$$

701 when converting to the log parameterization, we obtain the full conditional for  $\xi$ ,

$$702 \quad [\xi|\cdot] \propto \mathcal{N}(\boldsymbol{\delta}_p|\mathbf{0}, \mathbf{I}_{\kappa_p} \otimes e^{2\xi}(\mathbf{H}'\mathbf{H})^{-1}) \cdot \mathcal{HT}(e^\xi|\phi_\omega, d_\omega) \cdot \xi \quad (\text{A.9})$$

703

704 As in the  $z$  updates, we use a normal random-walk proposal  $[\xi^*|\cdot] = \mathcal{N}(\xi, R_\xi)$ , where  $R_\xi$   
 705 is adaptively tuned throughout the MCMC run in the way as the  $\mathbf{z}$  updates. With regards  
 706 to  $\sigma$ , the  $\theta$  parameter is updated in an identical fashion with the full conditional distribution  
 707 given by

$$708 \quad [\theta|\cdot] \propto \mathcal{N}(\mathbf{z}|\mathbf{X}\boldsymbol{\beta} + \mathbf{K}_p\boldsymbol{\delta}_p, e^\theta\mathbf{I}) \cdot \mathcal{HT}(e^\theta|\phi_\sigma, d_\sigma) \cdot \theta \quad (\text{A.10})$$

709 and adaptive random walk proposal distribution  $\mathcal{N}(\theta^*|\theta, R_\theta)$ .

## 710 **A.6 Updating $p$ and $\alpha$**

711 The update of  $p$  was described in the main portion of the paper, therefore we omit it here  
 712 and refer the reader to Section 2.2 for details.

713 The CRP parameter  $\alpha$  is updated through an MH step with the previously described  
 714 adaptive random walk proposal on  $\log \alpha$ . The full conditional distribution is given by

$$715 \quad [\alpha|\cdot] \propto \mathcal{CRP}(p|\alpha) \cdot \mathcal{G}(\alpha|a, b). \quad (\text{A.11})$$



716 However, as with all of the positive valued parameters, we choose to reparameterize to the log  
717 scale to make use of the adaptive random walk proposal distribution. So, the full conditional  
718 distribution for  $\log \alpha$  is

$$719 \quad [\log \alpha | \cdot] \propto \mathcal{CRP}(p|\alpha) \cdot \mathcal{G}(\alpha|a, b) \cdot \log \alpha. \quad (\text{A.12})$$

720 The same adaptive procedure was used with an MH acceptance step to sample the full  
721 conditional distribution.

## 722 Appendix B: Additional results for fish survey abun- 723 dance model

Table A.2: Results for species-specific Zero-inflated Poisson (ZIP) mixture parameters,  $\gamma_i$ . The ‘Estimate’ column is the posterior mode estimate and the ‘CI’ columns are the upper and lower 0.95 highest probability density interval values. The mixture probabilities represent the probability that a given species is unavailable for surveying in a particular survey.

	Estimate	Lower CI	Upper CI
<i>Albatrossia pectoralis</i>	0.20	0.03	0.44
<i>Avocettina infans</i>	0.52	0.27	0.74
<i>Bathylagus pacificus</i>	0.04	0.00	0.20
<i>Chauliodus macouni</i>	0.03	0.00	0.17
<i>Coryphaenoides cinereus</i>	0.14	0.00	0.46
<i>Diaphus theta</i>	0.18	0.04	0.33
<i>Lampanyctus jordani</i>	0.08	0.00	0.24
<i>Leuroglossus schmidti</i>	0.01	0.00	0.07
<i>Lipolagus ochotensis</i>	0.13	0.02	0.28
<i>Lycodapus fierasfer</i>	0.43	0.20	0.69
<i>Lycodapus poecilus</i>	0.58	0.35	0.79
<i>Macropinna microstoma</i>	0.07	0.00	0.36
<i>Melamphaes lugubris</i>	0.18	0.00	0.40
<i>Nannobranchium regale</i>	0.54	0.28	0.75
<i>Poromitra crassiceps</i>	0.03	0.00	0.28
<i>Pseudobathylagus milleri</i>	0.28	0.00	0.56
<i>Sigmops gracilis</i>	0.37	0.03	0.66
<i>Stenobranchius leucopsarus</i>	0.01	0.00	0.07
<i>Stenobranchius nannochir</i>	0.04	0.00	0.15
<i>Tactostoma macropus</i>	0.32	0.00	0.57

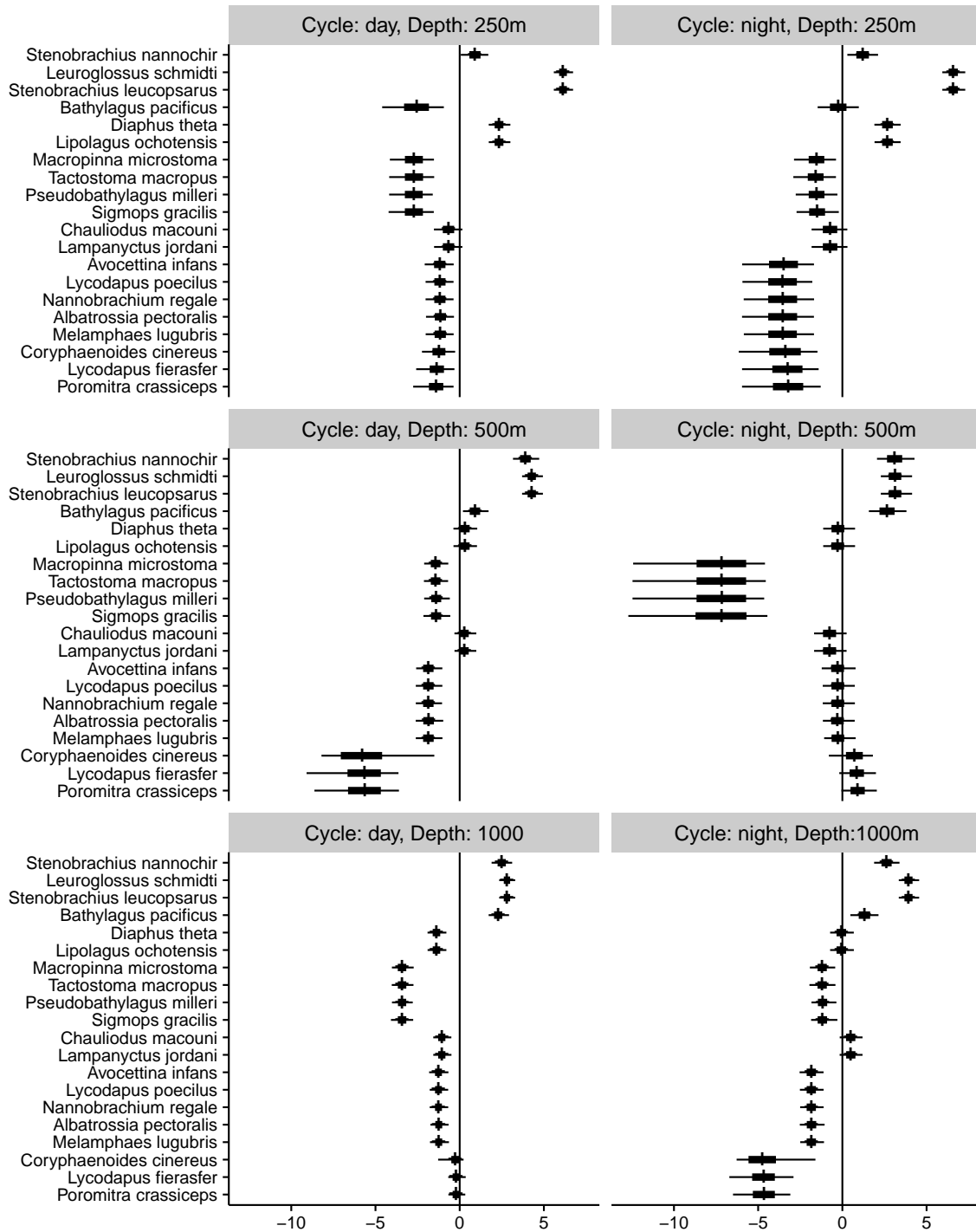


Figure B.1: Species-specific  $\delta$  estimates,  $\bar{\delta}_i$ , for each level of cycle (day or night), and depth (250, 500, or 1000 m).

724 **Appendix C: Mesopeleagic fish survey occurrence mod-**  
 eling  
 725

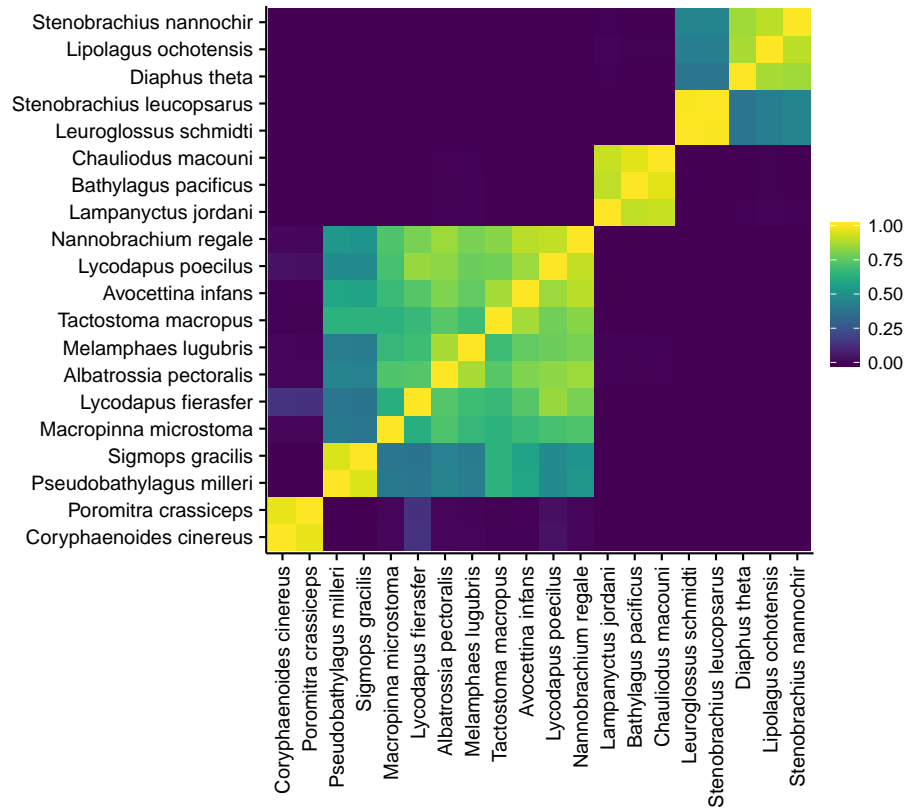


Figure C.1: Estimated probability of joint guild membership for each of the fish species in the trawl survey.

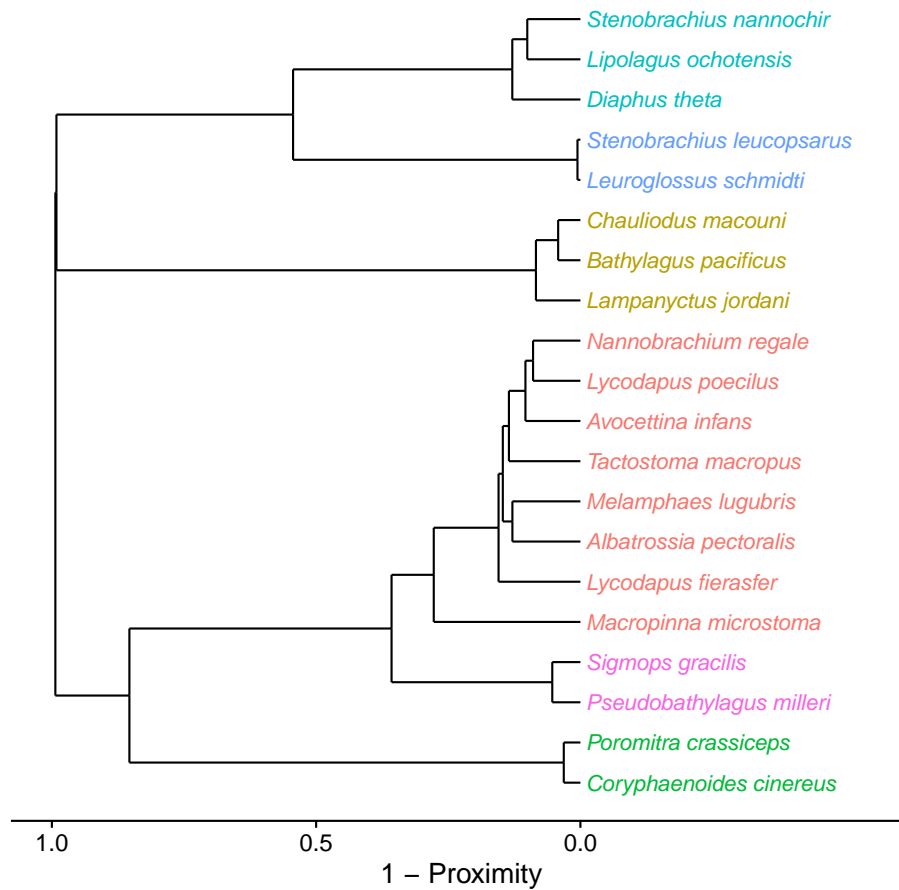


Figure C.2: Clustering of trawl survey fish species based on the estimated probability of joint guild membership.

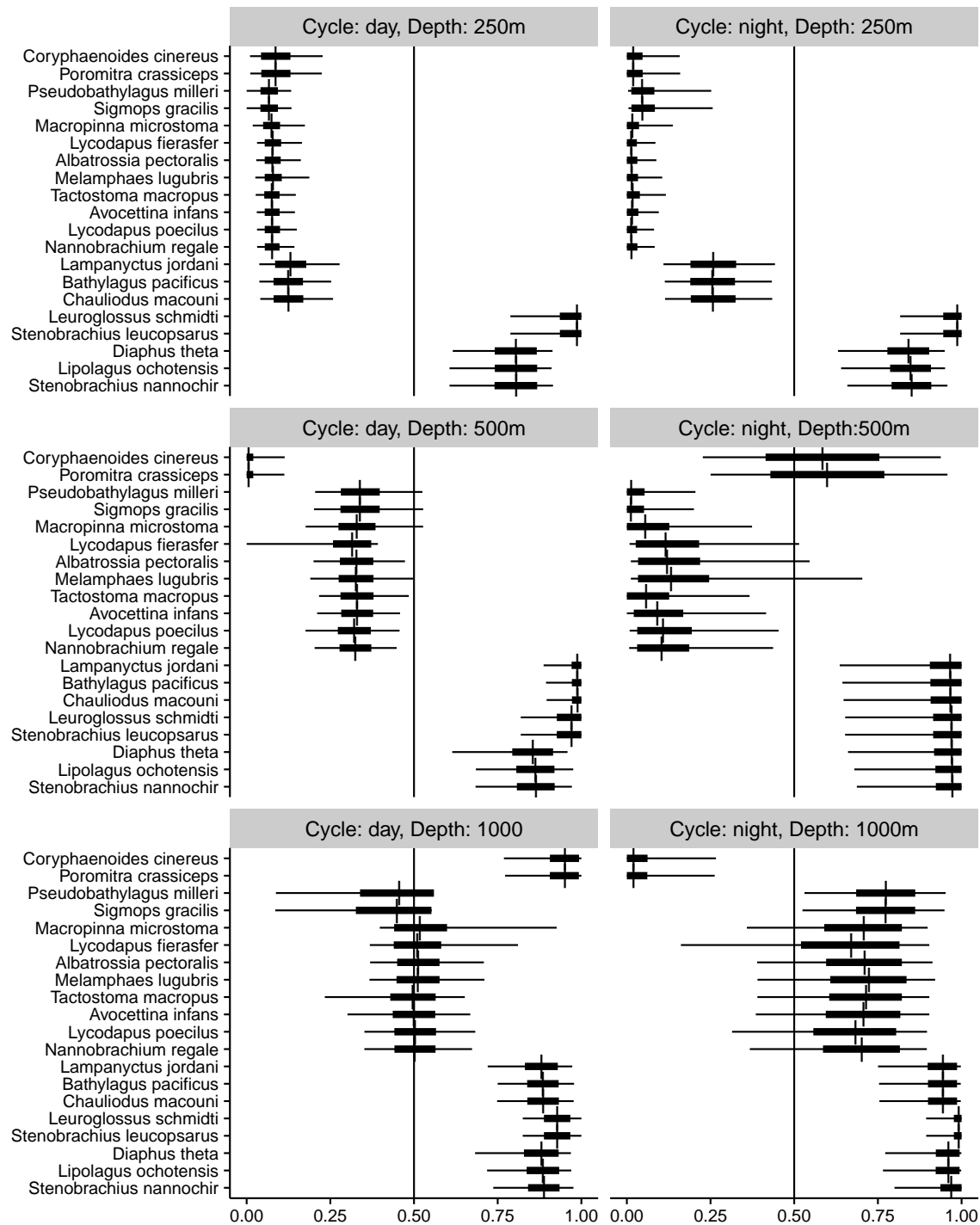


Figure C.3: Species-specific predictions of occurrence for each level of cycle (day or night), and depth (250m, 500m, or 1000m).